Summer 2008

Evaluation of SU8 and ruthenium oxide materials for microfluidic devices

Margaret Theresa Audrain

Department:

EVALUATION OF SU8 AND RUTHENIUM OXIDE MATERIALS FOR MICROFLUIDIC DEVICES

by

Margaret T. Audrain

A THESIS

Presented to the Faculty of the Graduate School of the

MISSOURI UNIVERSITY OF SCIENCE AND TECHNOLOGY

In Partial Fulfillment of the Requirements for the Degree

MASTER OF SCIENCE IN MATERIALS SCIENCE AND ENGINEERING

2008

Approved by

M. J. O'Keefe, Advisor
C. Kim
F. S. Miller

PUBLICATION THESIS OPTION

This thesis consists of the following two articles that will be submitted for publication as follows:

Pages 16-30 are intended for submission to the JOURNAL OF MICROMECHANICS AND MICROENGINEERING

Pages 31-48 are intended for submission in THIN SOLID FILMS

ABSTRACT

This thesis investigates two materials, SU8 photoresist and RuO_2, for possible incorporation into a self-calibrating microfluidic biosensor. The negative, epoxy based photoresist SU8 has been widely used in the fabrication of micro-electro-mechanical systems (MEMS) devices. This is due to its many desirable features that make it a suitable material for a wide variety of MEMS applications. The effects cross-linking (exposure dose) and bonding time have on bond strength and plasma modification of the SU8 surface were investigated as well as the bond strength of etched SU8. It was shown that adhesive bonding was an effective method of bonding, with bond strengths of 1500 psi possible. Plasma etching of SU8 was shown to significantly modify the surface while having a detrimental effect on bond strength. High oxygen plasma etching produced a hydrophilic SU8 surface, while CF_4 etching produced a hydrophobic surface. In both cases, the surface modification was shown to be temporary. Another important aspect of the biosensor is the electrode material. Ruthenium oxide (RuO_2) was examined because it has been shown to have much potential for use as an electrode. The resistivity, crystallinity and adhesion of reactively sputter deposited RuO_2 thin films to SU8 as a function of oxygen in the sputtering gas was investigated. It was found that both a change from Ru to RuO_2 films and a transition in preferred crystal orientation of RuO_2 in the films occurred as oxygen content in the film increased. It was shown that resistivity of RuO_2 is related to the amount of oxygen in the film. Film stress was shown to have a large impact on adhesion to SU8 and for this reason films produced in a moderate oxygen environment are suggested for use as an electrode material.

ACKNOWLEDGMENTS

I would like to thank my advisor, Dr. Matt O'Keefe, for all his guidance over the last two years. I would also like to thank Dr. Miller and Dr. Kim for taking the time to serve on my committee.

Many thanks to my lab-mates James Reck and Travis McKindra for teaching me in the lab, assisting me in analyzing results, and helping me with my homework. It would have been a much harder transition into materials engineering if not for you both.

I would like to thank the National Institute of Health for funding the project. I would also like to thank Jeff Wight and Eric Bohannan for technical services.

I would like to thank my parents and brothers for supporting me through my education and being a foot in my back when I needed them to be.

TABLE OF CONTENTS

LIST OF ILLUSTRATIONS

LIST OF TABLES

1. INTRODUCTION

1.1 MICROFLUIDIC DEVICE

Any device intended for long-term in vivo applications has to fulfill rigorous biocompatibility and biostability requirements. It should not induce toxicity in the surrounding tissues, and should not damage the local tissue due to induced mechanical stresses. The implant must tolerate long-term exposure to the physiological environment, as well as resist the impact of the surrounding tissue on its function. Important characteristics of materials for biological applications include lack of toxicity, lack of immunogenicity (the tendency to induce an immune response), biodegradability (fast, slow, or absent), adhesiveness (or lack thereof) to bio-macromolecules and cells, and appropriate mechanical properties (modulus and strength) [1, 2]. Additional requirements for a material to be used as microfluidic structures are the ability to reproduce and maintain microstructure and the ability to form a pressure-tight seal with itself and other components [2].

This thesis investigates two materials, SU8 photoresist and RuO_2, for possible incorporation into a self-calibrating microfluidic biosensor. Figure 1 shows a schematic of the self-calibrating biosensor that is being developed. Most biosensors drift and degrade over time, making calibration difficult. A self-calibrating biosensor would allow for continuous monitoring with minimal intervention. SU8 has been used to form microchannels, which are simple yet essential elements in microfluidic systems [3], while RuO_2 is being considered as an electrode material.

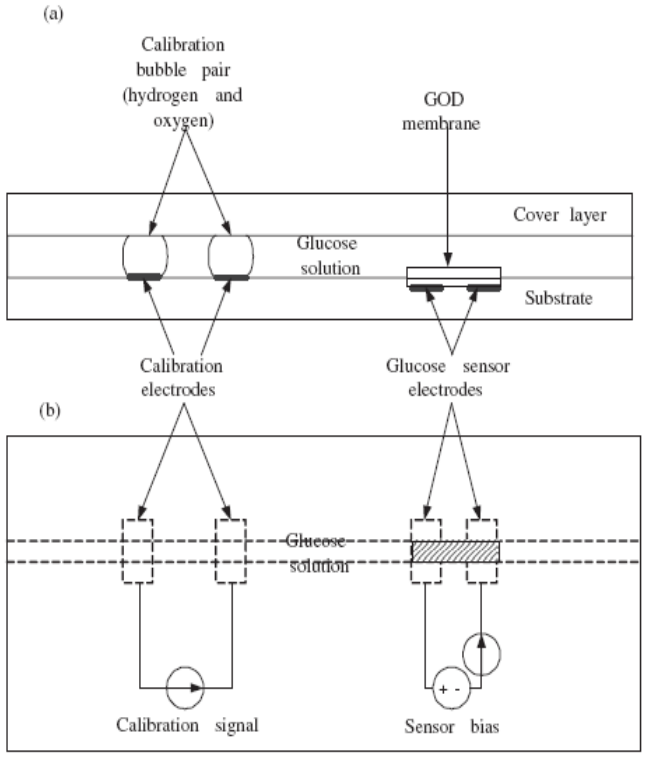

Figure 1.1 Schematic of self-calibrating biosensor

1.2 SU8

The negative, epoxy based photoresist SU8, shown in Figure 2, has been widely used in the fabrication of micro-electro-mechanical systems (MEMS) devices. This is due to its many desirable features that make it a suitable material for a wide variety of MEMS applications, including mechanical reliability, biocompatibility [4, 5], chemical resistance to electrolytes, patternability and low cost [4, 6-8]. In a study undertaken to investigate many types of photoresists, SU8 was found to be a suitable material to create three-dimensional structures such as a microfluidic device [9]. Unlike many thick photoresists, SU8 is mechanically strong and optically transparent [10], which allows

patterning of up to 2mm thick layers with high aspect ratios (up to 66:1) [11]and vertical side walls. In addition, it does not exhibit the swelling that is prevalent in many negative photoresists. Structures made completely of SU8 have good thermal and electrical isolation, which are desirable in the fabrication of microchannels [11]. SU8 has a few potential drawbacks, such as its high coefficient of thermal expansion (CTE, 52 ppm/K) that could cause stresses to substrates if the SU8 is used with materials with very different CTE values at high temperatures [12]. Also, cracks caused by tensile stress can form when processing SU8 [13].

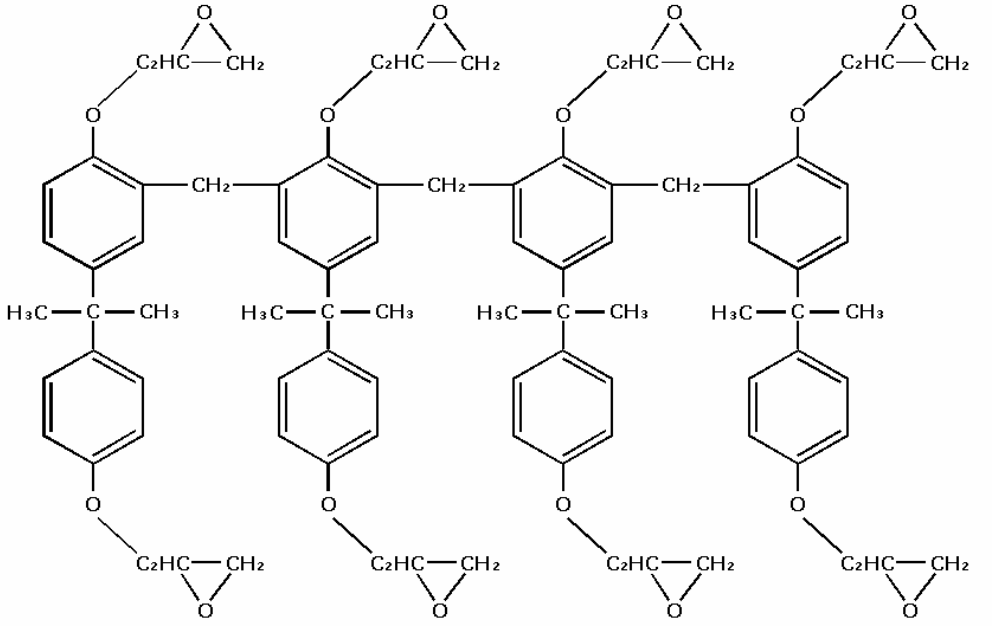

Figure 1.2 Basic SU8 model showing the eight epoxy groups

Resin, solvent and photoactive compound are the three main parts of SU8 but the properties are very sensitive to the processing conditions. The first step, spin-coating, is critical, as thickness and topography of the material corresponds to the spin-coating process [9]. Most of the solvent, around 80 wt%, is removed from the resist layer during

a soft-baking step at moderate heat (65 – 90°C) after spin-coating [12, 14]. Since a fixed solvent content leads to good resolution and high aspect ratio [14], care must be taken to use the appropriate soft-baking conditions. The resin is made photosensitive through the addition of an onium salt, which acts as a photo-acid generator. When exposed to UV light, the onium salt decomposes and generates a strong acid. This acid acts as a catalyst and initiates polymerization by ring-opening and subsequent cross-linking the epoxy groups [13]. The rate of cross-linking is related to the concentration of the acid catalyst. At low ultraviolet (UV) light dosage (<300 mJ/cm^2), not all of the photo-acid generator can change to acid, causing the concentration of the catalyst to be low. If the concentration of the acid is low, the cross-linking reaction will be kinetically slow. In addition, coatings exposed to higher UV dosages are more homogeneous than coatings exposed to low UV dosage [6, 12].

One aspect of SU8 processing in need of further investigation is its bonding capabilities. Since SU8 cannot be fabricated to have overhanging parts and open channels are not useful for fluidic applications due to intolerance to pressure and fast evaporation of samples, bonding is necessary to form enclosed channels [10]. It has been demonstrated that three dimensional interconnected enclosed channels could be fabricated by bonding SU8 [15]. To create enclosed microchannels, an effective and reliable bonding technique is required [6].

Bonding of SU8 is adhesive in nature where the polymer itself is used as the bonding layer. The epoxy produces very high bonding strength without requiring high pressures or temperatures during bonding [9]. Bonding strengths of SU8 to SU8 between 1100-1900 psi have been reported[16]. Adhesive bonding has several advantages: 1) the

bonding temperature can be relatively low (below 100°C); 2) many kinds of materials can be joined, such as polyimides, epoxies, thermoplast adhesives and photoresists; 3) the adhesive tolerates particles and structures on the wafer surface with diameters smaller than the polymer thickness; 4) high bonding strengths along the order of 1000 psi can be achieved at a low cost. Potential limitations include temperature stability and long-term material stability. Degradation of material properties can be caused by moisture uptake, temperature changes, and mechanical and chemical impacts [10, 17, 18].

Previous studies have shown that bonding temperature and bonding pressure are important parameters in having a good bond while maintaining clear fluidic channels [17]. If the bonding temperature is too low, SU8 will not be soft enough to make contact with the entire bonding area. If the bonding temperature is too high, significantly higher than the glass transition temperature of 50-55°C, SU8 will flow into and block the microchannels[3]. However, at higher bonding temperatures and forces, the bonding strength becomes nearly constant [16]. The optimum bonding temperature has been previously reported to be between 45 and 50°C [17]. Bonding pressure is an important parameter because if it is too low, cavities between substrates are not sealed, creating voids; if it is too high, the microstructure could be destroyed while bonding [9].

Processing conditions can significantly impact bond strength. Spin coating related problems, such and bubbles and thickness irregularities, cause problems in bonding, especially in the case of edge beads [6, 11]. UV exposure and post-exposure bake (PEB) conditions control the amount of cross-linking. Control of cross-linking is needed for good adhesive and mechanical properties of the bond layer. The last cross-

linking step needs to be done during bonding. This means that the polymer layer has not been fully cross-linked before bonding [6].

There are advantages to bonding both exposed and unexposed SU8. Exposed SU8 has low bond strength, but there is very little likelihood of collapse since the epoxy is cross-linked [19]. Unexposed SU8 has higher bond strength; however, it can flow into and block microchannels during bonding. Studies have shown that SU8 can be partially pre-baked and bonded with another wafer by applying pressure and heat [17]. Using a partially baked, partially exposed SU8 layer could provide the best solution as it has some mechanical strength but is not fully cured.

The surface chemical structure of SU8 after exposure consists of aromatic rings and methyl functional groups, which results in a large water contact angle. This can create difficulty with fluid injection into microchannels [20]. If the surface of the channel is hydrophilic, the capillary pressure can be used as the only means to direct the liquid through the channels and the need for external pumps can be avoided [8]. Previous work has used cericammoniumnitrate (CAN) to make the SU8 surface hydrophilic. However, CAN is corrosive and hazardous for humans [8].

A safer technique to modify the SU8 surface is oxygen plasma etching. It is well known that oxygen plasma etching can remove most solidified photoresists and that the removal rates can be enhanced when fluorinated gases are added to the oxygen plasma. Even a small percentage of fluorinated gas can increase the etching rate for many resists because atomistic fluorine reactions produce reactive sites on the polymer backbone and small amounts of fluorine increase the concentration of atomic oxygen in the plasma [4].

Using fluorine etch gases limits the materials that can be used as a mask; however, some metals, such as gold and aluminum, have had good results [21].

Studies show that contact angles on SU8 surfaces decrease with increasing O_2 plasma time [22]. It has been reported that the hydrophobic surface has been modified to hydrophilic within 10 seconds of plasma time [22]. A longer plasma exposure time also leads to better surface uniformity, increased surface energy, and decreased contact angles [22]. Increased plasma intensity also causes greater surface roughness, which leads to greater wetting capabilities. The plasma exposure affects the surface chemistry, increasing the oxygen levels while decreasing the carbon levels, resulting in an activated surface [23].

The first paper investigates the effects cross-linking (exposure dose) and bonding time have on bond strength and plasma modification of the SU8 surface. In addition, the bond strength of etched SU8 is tested since it is important for incorporation in a microfluidic device.

1.3 RuO_2

Ruthenium oxide (RuO_2) is a material that has been shown to serve as an excellent electrode material [24]. This is because of its low resistivity, high thermal stability, good corrosion resistance and diffusion barrier properties [24-31]. In addition, ruthenium metal oxidizes very slowly, but once formed, RuO_2 is one of the most chemically stable oxides [27, 30]. Single crystalline RuO_2 shows metallic behavior in electrical and optical properties [30].

RuO_2 belongs to the class of transition metal oxides that crystallize in the tetragonal rutile structure, a body-centered tetragonal structure, shown in Figure 3, with a ruthenium atom in each of two sublattices [28, 32]. RuO_2 thin films often exhibit preferred crystal orientation that is dependent on processing conditions [25].

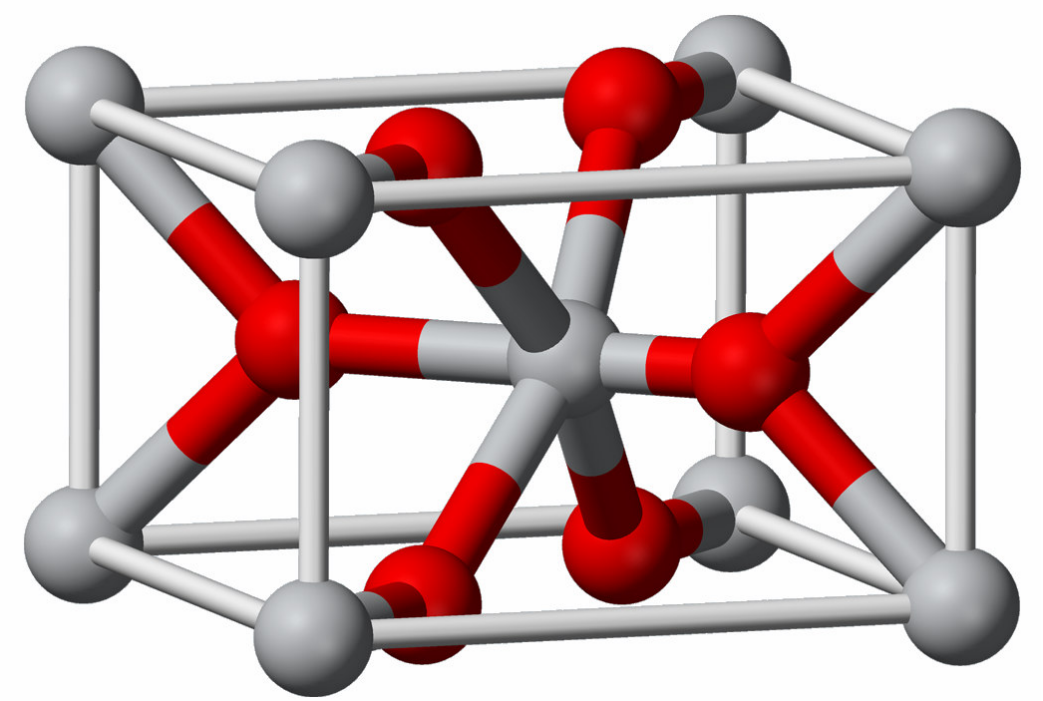

Figure 1.3 Tetragonal rutile structure

It is well known that the electrical, optical and microstructural properties of materials in thin film forms depend on the deposition techniques and deposition conditions [30, 33, 34]. Thin films of RuO_2 have been prepared using many methods, including reactive sputtering [27] and chemical vapor deposition (CVD) [27, 34]. Films were prepared using DC sputtering in this investigation because of available equipment and good results from other groups using this method. The microstructure and electrical properties of RuO_2 thin films can be controlled by varying sputtering conditions [35].

Oxygen concentration is an important parameter, controlling film resistivity [27] and preferred crystalline orientations [26]. As-deposited RuO_2 films remain stoichiometric as determined by both Rutherford backscattering (RBS) and x-ray diffraction (XRD) when the oxygen content is varied from 25-100%, confirming RuO_2 as the only stable oxide of Ru formed. Increased oxygen partial pressure causes an increase of oxygen content in the film until saturation is reached [33, 35]. Increasing the oxygen partial pressure also increased the grain size of the RuO_2 film [33]. The stresses and microstructure, however, vary considerably with the amount of oxygen in the sputtering environment [36]. Oxygen concentration in the sputtering gas effects the surface morphology, crystallinity and chemical binding state of oxygen atoms in the films [31].

Deposition rates depend on processing parameters; however, it has been reported that a change in deposition rate occurs as the oxygen partial pressure increases. The variation of the deposition rate is thought to be caused by the difference in reaction processes. In the high deposition rate region, when lower oxygen partial pressures still form RuO_2, the Ru target is in a metallic state. Ru atoms sputtered from the metal target react with oxygen at the substrate surface and RuO_2 films are deposited (metallic target mode). A high deposition rate causes the films to not crystallize completely, and some oxygen atoms might not be bonded with Ru atoms. Consequently, these films have higher electrical resistivities. In the low deposition rate region, the high oxygen partial pressure region, a Ru-oxide layer is formed at the target surface and RuO_2 films are deposited by the sputtering of Ru oxide (oxide target mode) [37]. At the lowest oxygen partial pressures, Ru films are produced [37]. At a constant total gas flow rate, a critical O_2 flow rate exists, which defines the minimum O_2 flow ratio for depositing RuO_2 films

[37]. Approximately twice as many oxygen molecules as sputtered Ru atoms must be introduced into the sputtering chamber in order to form RuO_2 films [37]; however, the oxygen content in the RuO_2 films is not sensitive the oxygen concentration in the Ar/O_2 sputtering gas [31] and RuO_2 films have been shown to remain stoichiometric by using 25-100% of oxygen in the Ar/O_2 sputtering gas [31, 36].

Film stress and surface properties have been investigated by many sources. As-deposited films have been found to be under a state of compressive stress for all deposition conditions [28]. It has also been shown that deposition under low oxygen contents can result in a higher amount of oxygen vacancies being produced in the films [28]. Annealing at low temperatures has been shown to make the film stress less compressive due to the movement of these vacancies [28]. In films deposited under very high oxygen content conditions (e.g. 100% O_2), the film stress has been shown not to remain compressive possibly because of reduced vacancies being present in the as-deposited films [28]. According to one study, the surface of films produced under lower oxygen partial pressure are slightly smoother than the surface of films produced at higher partial pressures [29]. With larger oxygen concentrations the surfaces exhibited clear granules with sharp angles [31].

Film resistivity has been shown to be dependent on deposition parameters such as substrate temperature, sputtering power, oxygen content, thickness of the films and annealing conditions [27, 28]. There appears to be an oxygen flow ratio where the films change from Ru to RuO_2 that is system and parameter dependent. Corresponding to this change, the film resistivity increases from around 20 μΩ-cm for the Ru films to much higher for the RuO_2 films [37]. The higher resistivity of as-deposited films is considered

as an indication of RuO_2 formation; incomplete oxidation of Ru results in much lower resistivity [35]. Resistivity values for RuO_2 vary widely from sources to source, from 40 to nearly 1000 μΩ-cm. The increase of resistivity along with the oxygen content suggests that the resistivity is largely affected by the amount of excess oxygen incorporated in the film [35]. Different electrical transport mechanisms have been identified for RuO_2 when in contact with various materials. In the case of high and low RuO_2 contects, metallic or ionic transport prevails. For intermediate concentrations, tunneling transport has been seen, mainly because of the densely packed microstructure [38].

The stresses in the as-deposited films in almost all cases were found to be compressive. The magnitude of both the as-deposited stress and resistivity were found to be strongly correlated to the microstructure of the films [28]. In most cases, annealing was found to result in an increase in the tensile stresses. This reduction in compressive stress has been attributed to grain growth at high temperatures. Associated with this grain growth was also a reduction in the resistivity of the films [28]. There is a distinct increase in grain size with increasing deposition temperature. The resistivity behavior with substrate temperature can be explained on the basis of the grain boundary scattering model [28]. If the predominant mechanism governing the resistivity is grain boundary scattering, then a larger grain size observed at higher deposition temperatures should provide a lower resistivity [25, 28].

For low oxygen partial pressures, the RuO_2 films exhibited a preferred orientation with RuO_2 (110) planes parallel to the Si substrate surface. When the RuO_2 film was deposited with higher oxygen concentration, the RuO_2 (110) peak became very weak or invisible and the preferred orientation changed to the RuO_2 (101) planes. Several other

sources reported similar results of changing preferred orientations from (110) planes to (101) planes with increasing oxygen concentration during RuO_2 sputtering [26, 34, 35, 37]. Huang et al believe that RuO_2 films sputtered with low oxygen content are not well crystallized, although the atoms may form a short-range periodic arrangement of RuO_2 (110) planes. As for the RuO_2 films sputtered with higher oxygen partial pressures, the films are all properly crystallized in the form of a rutile structure. The difference in crystallinity should be a key factor for the different resistivity values of the RuO_2 films sputtered with various oxygen concentrations [31]. It has been shown that (110) RuO_2, which is the preferential orientation in bulk RuO_2, is grown in the films with near stoichiometric oxygen composition, while preferential (101) grain growth occurs in the film with oxygen concentration near saturation [35].

The resistivity values vary widely from source to source, dependent on sputtering system and parameters. The purpose of the second paper is to determine the resistivity and crystallinity of as-deposited RuO_2 thin films reactively sputtered at 200W in an Ar/O_2 plasma without external substrate heating. In addition, the adhesion of RuO_2 thin films to the cured photoresist SU-8 is examined for potential use in a microfluidic device.

References

1. Oh, K.W., et al., *A low-temperature bonding technique using spin-on fluorocarbon polymers to assemble microsystems.* Journal of Micromechanics and Microengineering, 2002. **12**(2): p. 187-191.
2. Stroock, A.D. and M. Cabodi, *Microfluidic biomaterials.* MRS bulletin, 2006. **31**(2): p. 114-119.
3. Tuomikoski, S. and S. Franssila, *Free-standing SU-8 microfluidic chips by adhesive bonding and release etching.* Sensors & Actuators: A. Physical, 2005. **120**(2): p. 408-415.
4. Hong, G., A.S. Holmes, and M.E. Heaton, *SU8 resist plasma etching and its optimisation.* Microsystem Technologies, 2004. **10**(5): p. 357-359.

5. Voskerician, G., et al., *Biocompatibility and biofouling of MEMS drug delivery devices.* Biomaterials, 2003. **24**(11): p. 1959-1967.
6. Blanco, F.J., et al., *Novel three-dimensional embedded SU-8 microchannels fabricated using a low temperature full wafer adhesive bonding.* Journal of Micromechanics and Microengineering, 2004. **14**(7): p. 1047-1056.
7. Jackman, R.J., et al., *Microfluidic systems with on-line UV detection fabricated in photodefinable epoxy.* Journal of Micromechanics and Microengineering, 2001. **11**(3): p. 263-269.
8. Nordstroem, M., et al., *Rendering SU-8 hydrophilic to facilitate use in micro channel fabrication.* Journal of Micromechanics and Microengineering, 2004. **14**(12): p. 1614-1617.
9. Pan, C.T., et al., *A low-temperature wafer bonding technique using patternable materials.* Journal of Micromechanics and Microengineering, 2002. **12**(5): p. 611-615.
10. Tuomikoski, S., *Fabrication of SU8 microstructures for analytical microfluidic applications.* Thesis Publication, Helsinki University of Technology, 2007.
11. Tuomikoski, S. and S. Franssila, *Wafer-Level Bonding of MEMS Structures with SU-8 Epoxy Photoresist.* Physica Scripta, 2004. **114**: p. 223-226.
12. Feng, R. and R.J. Farris, *Influence of processing conditions on the thermal and mechanical properties of SU 8 negative photoresist coatings.* Journal of Micromechanics and Microengineering, 2003. **13**(1): p. 80-88.
13. Anhøj, T.A., et al., *The effect of soft bake temperature on the polymerization of SU-8 photoresist.* J. Micromech. Microeng. 2006. **16**(9): p. 1819-1824.
14. Zhang, J., et al., *Polymerization optimization of SU-8 photoresist and its applications in microfluidic systems and MEMS.* J. Micromech. Microeng, 2001. **11**(1): p. 20–26.
15. Peng, Z.C., et al., *Interconnected multilevel microfluidic channels fabricated using low-temperature bonding of SU-8 and multilayer lithography.* Proceedings of SPIE, 2005. **5718**: p. 209.
16. Bilenberg, B., et al., *PMMA to SU-8 bonding for polymer based lab-on-a-chip systems with integrated optics.* Journal of Micromechanics and Microengineering, 2004. **14**(6): p. 814-818.
17. Li, S., et al., *Fabrication of micronozzles using low-temperature wafer-level bonding with SU-8.* Journal of Micromechanics and Microengineering, 2003. **13**(5): p. 732-738.
18. Niklaus, F., et al., *Low-temperature full wafer adhesive bonding.* Journal of Micromechanics and Microengineering, 2001. **11**: p. 100-107.
19. Ruano-López, J.M., et al., *A new SU-8 process to integrate buried waveguides and sealed microchannels for a Lab-on-a-Chip.* Sensors & Actuators: B. Chemical, 2006. **114**(1): p. 542-551.
20. Wu, C.L., M.H. Chen, and F.G. Tseng, *SU-8 hydrophilic modification by forming copolymer with hydrophilic epoxy molecule.* 7th lnternational Conference on Miniaturized Chemical and Biochemical Analysts Systems, 2003: p. 5–9.
21. Mischke, H., G. Gruetzner, and M. Shaw, *Plasma etching of polymers like SU8 and BCB.* Proceedings of SPIE, 2003. **4979**: p. 372.

22. Chung, C.K. and Y.Z. Hong, *Surface modification of SU8 photoresist for shrinkage improvement in a monolithic MEMS microstructure.* Journal of Micromechanics and Microengineering, 2007. **17**(2): p. 207-212.
23. Walther, F., et al., *Stability of the hydrophilic behavior of oxygen plasma activated SU-8.* Journal of Micromechanics and Microengineering, 2007. **17**(3): p. 524-531.
24. Kim, H.K., et al., *All solid-state rechargeable thin-film microsupercapacitor fabricated with tungsten cosputtered ruthenium oxide electrodes.* Journal of Vacuum Science & Technology B: Microelectronics and Nanometer Structures, 2003. **21**: p. 949.
25. Hong, S.K., *Stress measurements of radio-frequency reactively sputtered RuO 2 thin films.* Journal of Applied Physics, 1996. **80**(2): p. 822.
26. Nougaret, L., et al., *Development of ruthenium dioxide electrodes for pyroelectric devices based on lithium tantalate thin films.* Thin Solid Films, 2007. **515**(7-8): p. 3971-3977.
27. Belkind, A., et al., *Optical properties of RuO2 films deposited by reactive sputtering.* Thin Solid Films, 1992. **207**(1-2): p. 242-247.
28. Desu, S.B., et al., *Stresses in sputtered RUOx thin films.* Thin Solid Films, 1999. **350**(1-2): p. 21-29.
29. Kim, H.K., et al., *Correlation between the microstructures and the cycling performance of RuO electrodes for thin-film microsupercapacitors.* Journal of Vacuum Science & Technology B: Microelectronics and Nanometer Structures, 2002. **20**: p. 1827.
30. Meng, L.J. and M.P. dos Santos, *A study of residual stress on rf reactively sputtered RuO2 thin films.* Thin Solid Films, 2000. **375**(1-2): p. 29-32.
31. Huang, J.H. and J.S. Chen, *Material characteristics and electrical property of reactively sputtered RuO2 thin films.* Thin Solid Films, 2001. **382**(1-2): p. 139-145.
32. Lister, T.E., et al., *Electrochemical and X-ray scattering study of well defined RuO2 single crystal surfaces.* Journal of Electroanalytical Chemistry, 2002. **524**: p. 201-218.
33. Sakiyama, K., et al., *Deposition and Properties of Reactively Sputtered Ruthenium Dioxide Films.* Journal of The Electrochemical Society, 1993. **140**: p. 834.
34. Lee, W., et al., *Implication of Liquid-Phase Deposited Amorphous RuO2 Electrode for Electrochemical Supercapacitor.* Electrochemical and Solid-State Letters, 2007. **10**: p. A225.
35. Lee, J., et al., *Effects of excess oxygen on the properties of reactively sputtered RuO2 thin films.* Journal of Applied Physics, 1995. **77**: p. 5473.
36. Krusin-Elbaum, L., M. Wittmer, and D.S. Yee, *Characterization of reactively sputtered ruthenium dioxide for very large scale integrated metallization.* Applied Physics Letters, 1987. **50**: p. 1879.
37. Abe, Y., et al., *Effects of O2 gas flow ratio and flow rate on the formation of RuO2 thin films by reactive sputtering.* Journal of Vacuum Science & Technology B: Microelectronics and Nanometer Structures, 2000. **18**: p. 1348.

38. Nicoloso, N., et al., *Conduction mechanisms in RuO_2 Composits*. Solid State Ionics, 1995. **75**: p. 211-216

PAPER 1

Effects of UV-exposure, bonding time and plasma treatment on bonding strength of SU8

M T Audrain, M J O'Keefe, C S Kim
Missouri University of Science and Technology, Materials Research Center, Rolla, MO, USA
E-mail: mjokeefe@mst.edu

Abstract. The negative, epoxy based photoresist SU8 has been widely used in the fabrication of micro-electro-mechanical systems (MEMS) devices in the past few years. This is due to its many desirable features that make it a suitable material for a wide variety of MEMS applications, including mechanical reliability, biocompatibility, chemical resistance to electrolytes, patternability and its low cost. This study investigates the effects cross-linking (exposure dose) and bonding time have on bond strength and plasma modification of the SU8 surface. Adhesive bonding of partially exposed SU8 to fully exposed SU8 was shown to be an effective method of bonding, with strengths over 1500 psi possible. The data indicate that exposure dose was a more significant parameter than exposure time on the bond strength of SU8 films. Exposure of SU8 to CF_4/O_2 plasmas was also studied. A range of oxygen concentration between 5% and 100% was tested, with high oxygen plasmas creating the most hydrophilic surface when tested with water. The stability of the etched surface was examined through wetting tests over a period of more than one month. For both hydrophobic and hydrophilic samples, the samples with the highest amount of fluorine in the plasma were the most stable over time. Based on the results, microfluidic channels with high bond strengths and hydrophilic surfaces can be realized if the proper processing parameters are selected.

1. Introduction

The negative, epoxy based photoresist SU8 has been widely used in the fabrication of micro-electro-mechanical systems (MEMS) devices in the past few years. This is due to its many desirable features that make it a suitable material for a wide variety of MEMS applications, including mechanical reliability, biocompatibility [1, 2], chemical resistance to electrolytes, patternability and low cost [1, 3-5].

One aspect of SU8 processing in need of further investigation is its bonding capabilities. Since SU8 cannot be fabricated to have overhanging parts and open channels are not useful for fluidic applications due to intolerance to pressure and fast evaporation of samples, bonding is necessary to form enclosed channels [6]. It has been demonstrated that three dimensional interconnected enclosed channels could be fabricated by bonding SU8 [7]. To create enclosed microchannels, an effective and reliable bonding technique is required [3].

Processing conditions can significantly impact bond strength. Spin coating related problems, such and bubbles and thickness irregularities, cause problems in bonding, especially in the case of edge beads [3, 8]. Ultraviolet (UV) exposure and post-exposure bake (PEB) conditions control the amount of cross-linking. Control of cross-linking is needed for good adhesive and mechanical properties of the bond layer. The last cross-linking step needs to be done during bonding so that the polymer layer has not been fully cross-linked before bonding [3].

There are advantages to bonding both exposed and unexposed SU8. Exposed SU8 has low bond strength, but there is very little likelihood of collapse since the epoxy is cross-linked [9]. Unexposed SU8 has higher bond strength; however, it can flow into and block microchannels during bonding. Studies have shown that SU8 can be partially pre-baked and bonded with another wafer by applying pressure and heat [10]. Using a partially baked, partially exposed SU8 layer could provide the best solution as it has some mechanical strength but is not fully cured.

The surface chemical structure of SU8 after exposure consists of aromatic rings and methyl functional groups, which results in a large water contact angle. This can

create difficulty with fluid injection into microchannels [11]. If the surface of the channel is hydrophilic, the capillary pressure can be used as the only means to direct the liquid through the channels and the need for external pumps can be avoided [5]. Previous work has used cericammoniumnitrate (CAN) to make the SU8 surface hydrophilic. However, CAN is corrosive and hazardous for humans [5].

A safer technique to modify the SU8 surface is oxygen plasma etching. It is well known that oxygen plasma etching can remove most solidified photoresists and that the removal rates can be enhanced when fluorinated gases are added to the oxygen plasma. Even a small percentage of fluorinated gas can increase the etching rate for many resists because atomistic fluorine reactions produce reactive sites on the polymer backbone and small amounts of fluorine increase the concentration of atomic oxygen in the plasma [1]. Using fluorine etch gases limits the materials that can be used as a mask; however, some metals, such as gold and aluminum, have had good results [12].

This study investigates the effects cross-linking (exposure dose) and bonding time have on bond strength and plasma modification of the SU8 surface. In addition, the bond strength of etched SU8 is tested since is important for incorporation in a microfluidic device.

2. Experimental Procedure

2.1 Fabrication of SU8 coated wafers

Silicon wafers (100 mm diameter) were cleaned by three minute immersion in acetone, methanol and de-ionized (DI) water, with air drying between each step. The

wafer was then spin dried and placed on a hotplate at 200°C for 5 minutes to dehydrate the wafer and improve the adhesion of SU8 films. Approximately 4 ml of SU8-2050 (Microchem Corporation) were deposited on the Si wafers and spun using a CEE Model 100 spin coater to attain the desired thickness as follows:

50 μm coating

- 500 rpm, 100 rpm/sec, 15 seconds
- 3000 rpm, 300 rpm/sec, 38 seconds

125 μm coating

- 500 rpm, 100 rpm/sec, 15 seconds
- 1600 rpm, 300 rpm/sec, 30 seconds

The first spin parameters given are to spread the SU8 across the Si wafers. The spin speed is then ramped up at 300 rpm/sec to the second spin speed, which controls the thickness of the coating. Pre-exposure baking was done at 65°C for 3 minutes and then 95°C for 20 minutes. The UV exposure was done using a Suss MA-BA 6 aligner. Exposure dose and post-exposure baking varied depending on if a fully cured or partially cured wafer was needed. A mask was placed on the wafers to photo-pattern those that were to be fully exposed. Depending on the intended use, the pattern was either small (1-2cm) squares or circles. The exposure dose for fully exposed SU8 was 300 mJ/cm^2. The exposure doses used for partially exposed SU8 varied (70-95 mJ/cm^2). Partially exposed wafers were not photo-patterned. After exposure, a post exposure bake was done for fully exposed wafers at 65°C for 5 minutes followed by 95°C for 10 minutes while partially exposed wafers were processed for 7 minutes at 50°C. After the post exposure bake, the wafer was gradually cooled to room temperature. The fully exposed wafers

were then developed for 6 minutes to remove unexposed material, rinsed with DI water, spin dried and baked at 200°C for 1 hour to remove any moisture.

2.2 Bonding Experiment

To test the bonding strength, 1 cm x 1 cm samples of 125 µm thick fully cured SU8 were bonded to larger samples of partially cured 50 µm thick SU8 (Figure 1). The exposure doses used for partially exposed SU8 were 70, 75, 80, 85 and 90 mJ/cm^2. Both the fully exposed and partially exposed wafers were scribed and broken into the test pieces. Samples from each exposure dose were bonded with fully cured samples for 30, 40, and 45 minutes using a Dynatex heat bonder at 25mTorr pressure. After bonding, epoxy coated pull studs were attached to the back of one of the samples and baked for 1 hour at 150°C. The samples were then allowed to cool for several hours to set the epoxy. The bond strength was tested using a Romulus tensile tester at a pull rate of 10 lb/s.

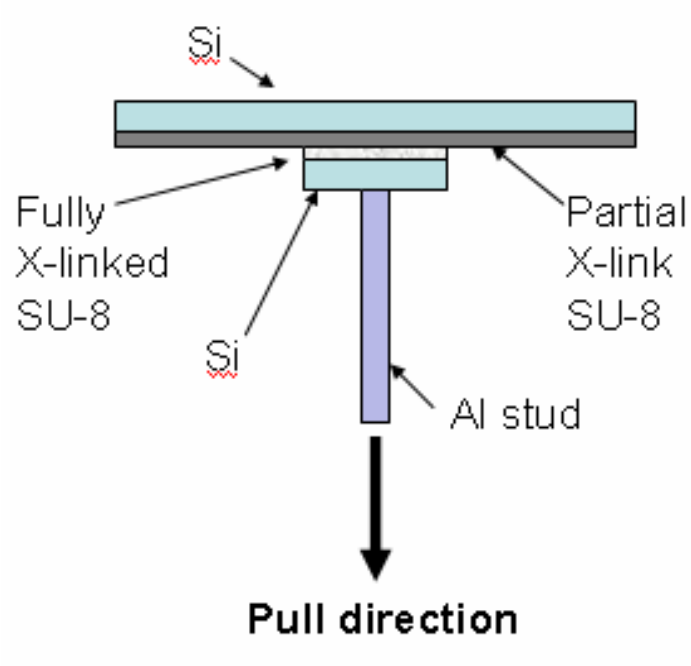

Figure 1. Schematic drawing of bond test sample

2.3 Contact Angles

Fully cured, 125 μm thick, circular samples were made to test the contact angles of etched SU8. A Plasma Etch PE-200 reactive ion etcher was used to etch all the samples with a CF_4/O_2 plasma (280W, 250 mTorr). A D-Optimal experiment was designed to test both etching time and percent oxygen. Five time levels were tested: 1, 30, 60, 90 and 120 seconds. Four oxygen plasma concentrations were tested: 5%, 30%, 70% and 100% oxygen, with the balance CF_4. A goniometer was used to measure the contact angle for water for each sample. Samples from the three longest etch times for each oxygen content were then tested once a day for over a month to determine the stability of the plasma exposed surface**.** A Kratos Axis 165 Photoelectron Spectrometer with Mg Kα radiation was used for x-ray spectroscopy analysis of both newly etched samples and 90 day old etched samples.

2.4 Bonding Etched Samples

The bond strength of plasma etched SU8 was tested by first preparing fully exposed 125 μm thick, 1cm x 1 cm sample pieces. Both high (100%) and low (5%) oxygen content plasmas were used and etched for 1, 30 and 60 seconds. Then, based on the results from the first bonding experiment, 50 μm thick, partially exposed samples were prepared with an exposure dose of 80 mJ/cm^2. The samples were then bonded in the same manner as previously described for 30 minutes.

3. Results and Discussion

3.1 Bonding Experiment

Two parameters were tested relating to bond strength: exposure dose and bond time. The average results from 5 samples are shown in Table 1.

Table 1. Average bond strength (psi)

Bond Time	Exposure (mJ/cm^2)				
	70	75	80	85	90
30 min	870 ± 320	950 ± 210	1374 ± 250	1114 ± 285	1225 ± 178
40 min	347 ± 72	1030 ± 212	1030 ± 300	1216 ± 337	720 ± 500
45 min	283 ± 220	1220 ± 166	1210 ± 250	762 ± 154	816 ± 355

Based on the data, the exposure dose has more of an effect than time, with the best results corresponding with an 80 mJ exposure. The lower exposure samples (70 mJ/cm^2) had the lowest average bond values of 300 to 800 psi while the high exposure samples (85, 90 mJ/cm^2) had bond strengths between 700 and 1200 psi on average. It is interesting to note that the longest bond time did not yield the highest bond strengths, except in the case of 75 mJ/cm^2. In the case of both 70 and 90 mJ/cm^2 the strongest bond strengths were produced with the shortest bond times, with the bond strengths for the longer bond times being much lower.

Statistical analysis of the data was performed using Design Ease software. ANOVA shows that the model is valid with no significant lack of fit. The most significant term in this study was found to be exposure dose. Figure 2 shows a graph of

the statistical results. From the graph, it is apparent that in general, the middle exposure doses produced the best results, with the peak being around 80 mJ/cm^2.

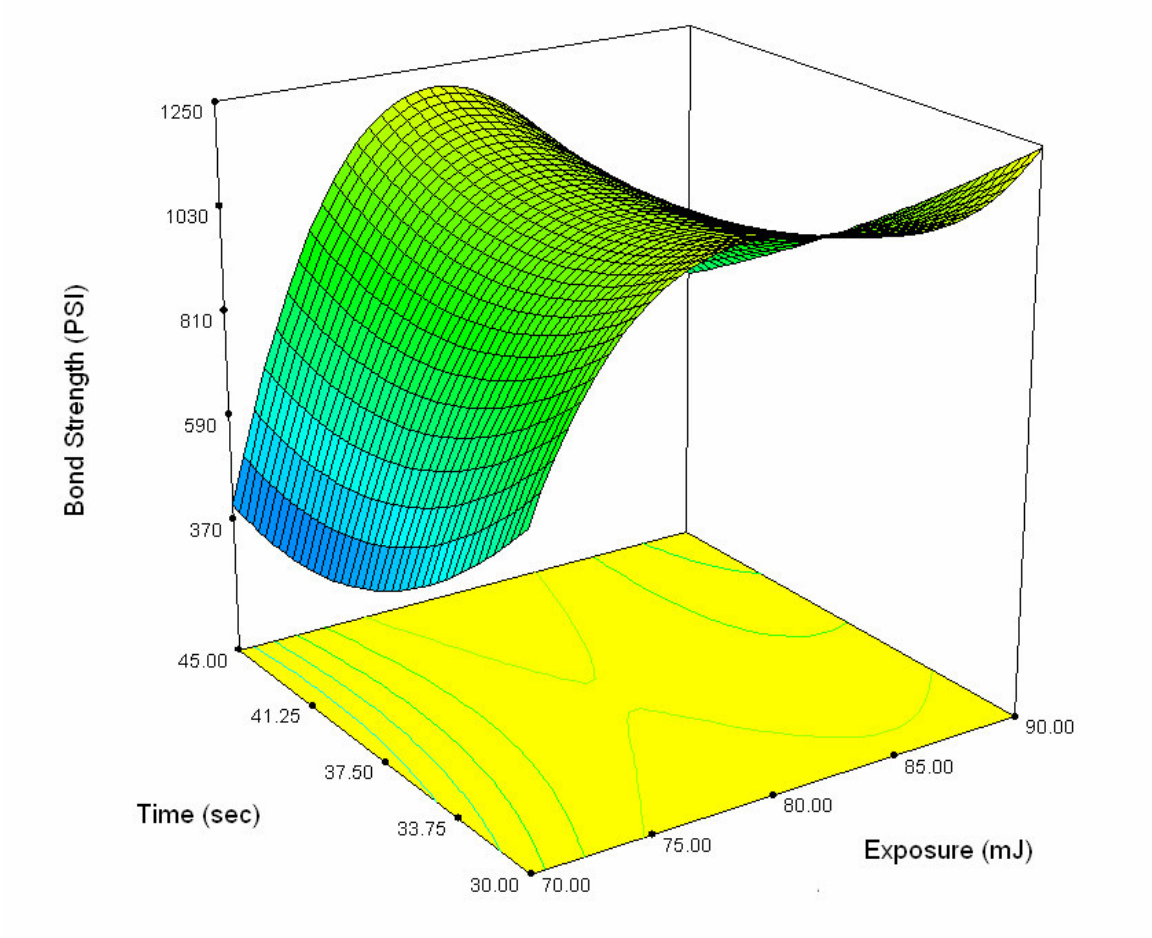

Figure 2. Statistical graph of bonding results showing the bond strength was more affected by exposure dose than bond time.

The fact that the significant factor in the bond test was the exposure dose is in agreement with the SU8 being a chemical bond instead of a mechanical bond. Studies done previously but not reported here show that the results were poor (<500 psi) when trying to bond outside of the range of exposure doses tested in this experiment. The reason the lower exposure doses do not bond well is most likely because there is not

enough initial cross-linking in the partially exposed film to bond with the fully exposed film. In the higher exposure doses, the bond strengths are not as high because there is too much cross-linking and the surface does not interact with the fully exposed substrate. The slight variations in bond strength with the different bonding times for 75-85 mJ/cm^2 are not significant and could be explained by slightly uneven topography of the film.

3.2 *Contact Angle*

3.2.1 Short Term Results

The oxygen content in the plasma had a significant impact on water contact angles. As shown in Table 2 and Figure 3, higher oxygen content led to low contact angle (hydrophilic) samples, where lower oxygen content led to high contact angle (hydrophobic) samples. Unetched SU8 has a contact angle of 73.8 ± 2.8 degrees.

Table 2. Contact Angle Results

	Etch Time				
% Oxygen	1	30	60	90	120
5	71.9 ± 15.9	93.6 ± 34.0	109.7 ± 8.3	101.0 ± 14.0	100.0 ± 2.5
30	72.8 ± 5.8	93.4 ± 5.6	99.8 ± 5.3	92.6 ± 3.9	91.7 ± 4.2
70	70.2 ± 7.5	26.0 ± 11.8	10.0 ± 2.8	14.4 ± 11.7	14.6 ± 13.7
100	67.2 ± 19.2	5.2 ± 1.9	5.1 ± 2.3	6.6 ± 1.8	5.1 ± 1.5

ANOVA results show that percent oxygen was a significant variable, whereas etch time was not. From the contour graph, it can be seen that a minimum etch time of around 20 seconds is needed to significantly change the SU8 surface.

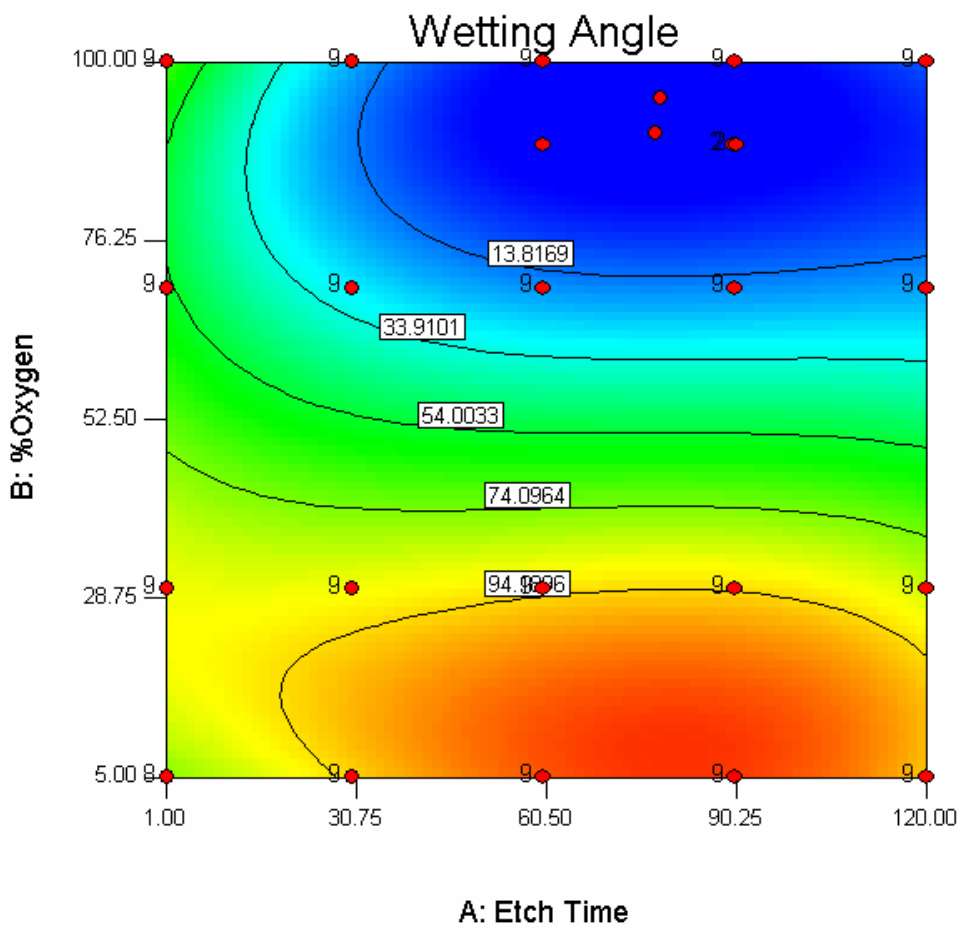

Figure 3 Contour graph of contact angle results. The red dots represent actual data points. The more red the color, the more hydrophobic the sample.

An explanation for high oxygen plasmas making the surface hydrophilic is that the etching most likely opens up the epoxy groups, which then can react with oxygen in the environment, forming hydrophilic –OH groups on the surface. With less oxygen in the environment, not as many –OH bonds will form, leading to a less hydrophilic surface. This is supported through analysis of XPS O 1s photoelectron spectra data as seen in Figure 4. From the binding energy the type of bond can be determined. In the top curve both oxygen peaks in the XPS data indicate that -OH groups formed on the SU8 surface.

However, after 90 days had passed, the bonds changed to more hydrophobic C=O bonds, seen in the bottom curve. The statistical analysis showed a significant lack-of-fit; however, with more data samples this would most likely change. To show the validity of the model, an optimization experiment was performed. The samples had the predicted contact angles based on oxygen content and etch time, which implies that the model is accurate.

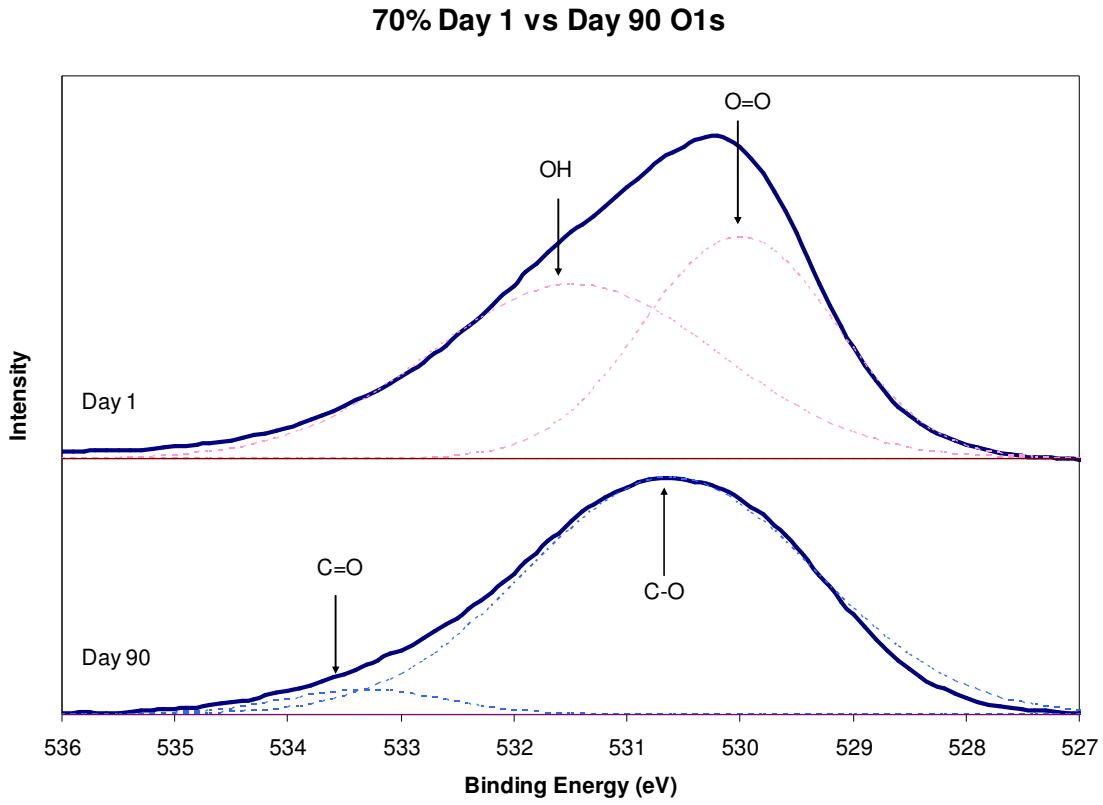

Figure 4. O 1s XPS spectra for SU8 surfaces from Day 1 and Day 90 after 70% oxygen/30% CF_4 plasma exposure of 30 minutes.

3.2.2 Long Term Results

For over one month samples from the three longest etch times for each oxygen plasma etch concentration were tested for contact angle each day. The results showed

that, again, etch time did not have a large impact on contact angle, since all three times resulted in similar contact angles over the test period for the varying oxygen contents in the plasma. The average wetting angles for the different oxygen contents are shown in Figure 5.

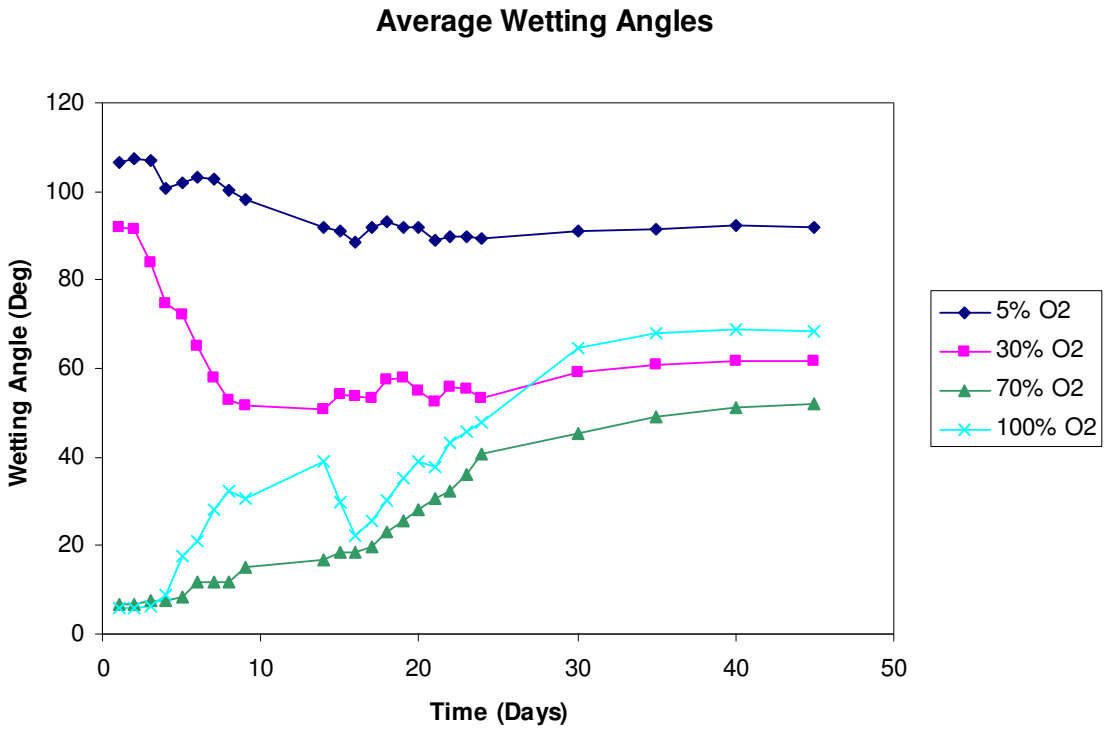

Figure 5. Time delay results for wetting angles

For both hydrophobic and hydrophilic samples, the samples with more fluorine than oxygen in the plasma were more stable over time, with the 5% oxygen content sample being the most stable and hydrophobic surface and with 100% oxygen content sample being the most unstable surface. From the graph, it seems as though the samples had a final contact angle between 60-80 degrees. It is possible that the repeated testing

led to a faster change in wetting angle, due to contamination of the outermost polymeric surface.

3.3 *Bonding Etched Samples*

The bond strength for etched SU8 samples is presented in Table 3. Both high and low oxygen plasma etched samples were tested. In general, exposure to CF_4/O_2 plasma significantly decreased the bond strength of the samples. The results were not very consistent, and the only sample that had bond strength comparable to un-etched SU8 was 5% oxygen for 1 second. It is not likely that plasmas with medium oxygen values would produce samples with better bonding capabilities as the contact angles were within the range tested. Based on these results, bonding etched SU8 does not appear to be a viable option. If etching is necessary, masking of the areas that need to be bonded would be needed.

Table 3. Average of 4 samples' bond strength after etching (psi)

	Etch Time (sec)		
% Oxygen	1	30	60
5	1010 ± 104	425 ± 163	0 ± 0
95	842 ± 367	763 ± 185	307 ± 62

4. Conclusion

The effect of UV exposure time and dosage, bonding time and plasma exposure on the adhesion and wafer contact angle of SU8 photoresist was investigated. Adhesive

bonding of partially exposed SU8 to fully exposed SU8 was shown to be an effective method of bonding, with strengths over 1200 psi possible. The data indicate that exposure dose was a more significant parameter than bonding time on the bond strength of SU8 films. Exposure of SU8 to CF_4/O_2 plasmas was also studied. A range of oxygen concentration between 5% and 100% was tested, with high oxygen plasmas creating the most hydrophilic surface when tested with water. The most likely reason high oxygen plasmas make the surface hydrophilic is that the etching would open the epoxy groups, which then can react with O_2 in the environment forming hydrophilic –OH groups on the surface. With less oxygen in the environment, fewer –OH will form, leading to a less hydrophilic surface. The stability of the etched surface was examined through wetting tests over a period of more than one month. For both hydrophobic and hydrophilic samples, the samples with the highest amount of fluorine in the plasma were the most stable over time. The samples had a final contact angle between 60-80 deg, similar to un-etched SU8 values. Based on the results, microfluidic channels with high bond strengths and hydrophilic surfaces can be realized if the proper processing parameters are selected.

5. Acknowledgements

This work was supported in part by the National Institute for Health, Grant 1R15EB006611-O1A1.

6. References

1. Hong, G., A.S. Holmes, and M.E. Heaton 2004 SU8 resist plasma etching and its optimisation. *Microsystem Tech.* **10** 357-359
2. Voskerician, G., et al. 2003 Biocompatibility and biofouling of MEMS drug delivery devices *Biomaterials*. **24** 1959-1967

3. Blanco, F.J., et al. 2004 Novel three-dimensional embedded SU8 microchannels fabricated using a low temperature full wafer adhesive bonding *J. Micromech. and Microeng*. **14** 1047-1056
4. Jackman, R.J., et al. 2001 Microfluidic systems with on-line UV detection fabricated in photodefinable epoxy *J. Micromech. and Microeng.* **11** 263-269
5. Nordstroem, M., et al. 2004 Rendering SU8hydrophilic to facilitate use in microchannel fabrication *J. Micromech. and Microeng.* **14** 1614-1617
6. Tuomikoski, S. 2007 Fabrication of SU-8 microstructures for analytical microfluidic applications *Thesis Publication Helsinki University of Technology.*
7. Peng, Z.C., et al. 2005 Interconnected multilevel microfluidic channels fabricated using low-temperature bonding of SU-8 and multilayer lithography. *Proceedings of SPIE* **5718** 209
8. Tuomikoski, S. and S. Franssila 2004 Wafer-Level Bonding of MEMS Structures with SU-8 Epoxy Photoresist. *Physica Scripta* **114** 223-226
9. Ruano-López, J.M., et al. 2006 A new SU-8 process to integrate buried waveguides and sealed microchannels for a Lab-on-a-Chip *Sensors & Actuators: B. Chemical* **114** 542-551
10. Li, S., et al. 2003 Fabrication of micronozzles using low-temperature wafer-level bonding with SU-8 *J. of Micromech. and Microeng.* **13** 732-738
11. Wu, C.L., M.H. Chen, and F.G. Tseng 2003 SU-8 hydrophilic modification by forming copolymer with hydrophilic epoxy molecule *7th international Conference on Miniaturized Chemical and Biochemical Analysts Systems*. 5–9.
12. Mischke, H., G. Gruetzner, and M. Shaw 2003 Plasma etching of polymers like SU8 and BCB *Proceedings of SPIE*. **4979** 372.

Paper 2

INFLUENCE OF OXYGEN ON REACTIVE SPUTTERING OF RUTHENIUM OXIDE

Margaret T. Audrain, Matthew O'Keefe, Chang-Soo Kim
Missouri University of Science and Technology– Rolla, Missouri, USA 65401
Contact Email: mjokeefe@mst.edu

Abstract

The resistivity and crystallinity of reactively sputter deposited RuO_2 thin films sputtered as a function of oxygen in the sputtering gas was investigated as well as the adhesion of RuO_2 thin films to cured SU8 photoresist. It was found that a change from Ru to RuO_2 films occurs between 20% and 30% oxygen in the plasma and a transition in the preferred crystal orientation in the films occurred between 80% and 90% oxygen. The change from Ru to RuO_2 occurring between 20 and 30% oxygen is further supported by AES results, which indicated a mixture of Ru and RuO_x in the 20% oxygen film. The resistivity values for films deposited with 30% to 60% oxygen were between 150-200 μΩ-cm. Adhesion was lower in films made with 60% oxygen and it is suggested that the best films for electrodes would be made in 40-50% oxygen environments where the adhesion values were above 1000 psi. Due to high film stress, films made with over 70% oxygen in the sputtering gas delaminated from the substrate.

Keywords: RF Sputtering, resistivity, ruthenium oxide

1. Introduction

Ruthenium oxide (RuO_2) has been investigated as an electrode material in many applications, such as in very large scale integrated circuits and ferroelectric thin films, because of its low resistivity, high thermal stability, good corrosion resistance and diffusion barrier properties [1-8]. In addition, ruthenium metal oxidizes very slowly, but once formed, RuO_2 is one of the most chemically stable oxides [3, 7]. Single crystalline RuO_2 shows metallic behavior in electrical and optical properties [7].

It is well known that the electrical, optical and microstructural properties of materials in thin film forms depend on the deposition techniques and deposition conditions [7, 9, 10]. Thin films of RuO_2 have been prepared using many methods, including reactive sputtering [3] and chemical vapor deposition (CVD) [3, 10]. The microstructure and electrical properties of RuO_2 thin films can be controlled by varying sputtering conditions [11].

Oxygen concentration in the plasma during sputtering is an important processing parameter as it influences film resistivity [3] and crystal orientation. The stresses and microstructure, however, vary considerably with the amount of oxygen in the sputtering environment [12]. Oxygen concentration in the sputtering gas does not affect the oxygen content in the film as much as changes the surface morphology, crystallinity and chemical binding state of oxygen atoms in the films [8].

Film resistivity has been shown to be dependent on deposition parameters such as substrate temperature, sputtering power, oxygen content, thickness of the films and annealing conditions [3, 4]. There appears to be an oxygen flow ratio where the films change from Ru to RuO_2 that is both deposition system and parameter dependent. Corresponding to this change, the film resistivity increases from around 20 μΩ-cm for metallic Ru films to much higher values for RuO_2 films [13]. The high resistivity of as-deposited films is an indication of RuO_2 formation; incomplete oxidation of Ru results in much lower resistivity [11]. Resistivity values for RuO_2 vary widely from sources to source. The increase of resistivity along with the oxygen content suggests that the resistivity is largely affected by the amount of excess oxygen incorporated in the film [11]. Table 1 shows representative sputtering conditions and the lowest resistivity values found for RuO_2 films in the literature and it is seen that there is a large divergence between the deposition parameters reported by different groups.

The amount of oxygen in the sputtering gas also influences the crystallography of the deposited films. Several sources reported results of changing preferred orientations from (110) planes to (101) planes with increasing oxygen concentration during RuO_2 sputtering [2, 10, 11, 13]. Huang et al believe that RuO_2 films sputtered with low oxygen content are not well crystallized although the atoms may form a short-range periodic arrangement of RuO_2 (110) planes. For RuO_2 films sputtered with higher oxygen partial pressures, the films are all properly crystallized in the form of a rutile structure. The difference in crystallinity has been reported to be a key factor for the different resistivity values of the RuO_2 films sputtered with various oxygen concentrations [8].

The purpose of this work was to determine the resistivity and crystallinity of DC reactively sputtered RuO_2 as a function of oxygen concentration in the sputtering gas. In addition, the adhesion of RuO_2 thin films to the cured photoresist SU8 was examined for potential use as an electrode material in a microfluidic device.

2. Experimental Procedure

RuO_2 films were deposited using a DC sputtering system and a ruthenium metal target in an oxygen and argon plasma. The substrates were silicon (Si) wafers and fully exposed photoresist SU8. The vacuum chamber was pumped down to a pressure of less than 4×10^{-6} mTorr prior to deposition. The target was presputtered (200 W DC power) with a shutter covering the substrate in an argon atmosphere for approximately 10 minutes to remove any surface oxide layer formed. The oxygen and argon gas mixture was then set for a total pressure of 5 mTorr and the gases were allowed to equilibrate prior to sputtering. Typical flow rates were around 25 sccm. Oxygen partial pressure was varied from 0 to 100 percent in 10 percent increments. The DC power during film deposition was 200 W and the deposition time was 10 minutes. Substrates were not heated during deposition.

After sputtering, film thickness was measured using an alpha step profilometer. Film resistivity was calculated using a four point probe. Film adhesion to SU8 was testing by attaching epoxy coated pull studs to the film, which were then baked for 1 hour at 150°C. The samples were then allowed to cool for several hours to set the epoxy. The film adhesion was tested using a Romulus tensile tester at a pull rate of 10 lb/s. A

physical electronics model 545 AES Spectrometer was used for Auger analysis with a beam voltage of 3 kV and an emission current of 1 mA. X-ray Diffraction (XRD) was performed using a Philips X-Pert diffractometer with copper Kα radiation.

3. Results and Discussion

3.1 Crystallography

Results from X-Ray Diffraction (XRD) show that with the parameters used, the transition from Ru to RuO_2 films occurred around 20% oxygen and was completed by 30% oxygen in the sputtering gas. The diffraction patterns for pure Ru, 20% and 30% RuO_2 is shown in Figure 1. The diffraction pattern for 10% oxygen (not shown) is the same as that for 0% oxygen, indicating a Ru film. The diffraction pattern of a RuO_2 film deposited with 50% oxygen is shown in Figure 2. The diffraction patterns for 40% and 60% oxygen (not shown) are the same as for the 50% oxygen. All of the diffraction peaks are identified as pertaining to stoichiometric ruthenium dioxide, with a preferred (110) orientation observed. In films deposited with oxygen partial pressures 70% and lower, the diffraction patterns are predominately (110) crystal structures. As the amount of oxygen in the sputtering gas increased up to 90% the diffraction peaks became broad and weak, as shown in Figure 3, indicating a fine grained crystal structure, which has also been reported by Kim, et al and Abe et al [6, 13]. The (101) crystal plane first becomes apparent in 50% oxygen films. Between 80% and 90% oxygen in the sputtering gas, the (101) crystal plane becomes dominant as seen when comparing Figures 3 and 4.

It was observed that in films deposited with greater than 70% oxygen the stress in the films was so high that delamination occurred after deposition. Therefore, films deposited under those conditions are not viable for use as an electrode material. For this reason, only the RuO_2 films with oxygen content lower than 70% were examined for resistivity and film adhesion.

3.2 Chemical Analysis

The composition of RuO_2 films deposited with 20% and 50% oxygen were examined using Auger Electron Spectroscopy (AES) to determine the atomic percent of both ruthenium and oxygen in the film. All three films had RuO_2 stoichiometry at the film surface, with approximately 30-40 atomic percent ruthenium and the balance oxygen. For the 20% oxygen film, shown in Figure 5, as the film depth increases, the amount of Ru was greater than the amount of oxygen. This indicates a film that is a mix of Ru and RuO_x, which supports the XRD data showing a transition from pure Ru to RuO_2 between 20% and 30% oxygen.

As expected from the XRD data, the film sputtered at 50% oxygen, shown in Figure 6, remained stoichiometric RuO_2 throughout the film. The atomic percent for ruthenium and oxygen remain consistently around 38 at% and 62 at%, respectively, at a film depth of 4 nm and greater. At the immediate film surface, there is more oxygen, but this was to be expected since the film was not kept in a vacuum prior to AES characterization.

3.3 Resistivity and Film Adhesion

Figure 7 presents the electrical resistivity of RuO_2 films with varying oxygen deposition percentages. Ru has a resistivity value of 7-8 μΩ-cm, which is the range the resistivity values for the 0% and 10% oxygen films encompasses. This indicates that both films are Ru and not an oxide. The 20% and 30% oxygen films are composed of a mixture of Ru and RuO_x, and have a higher resistivity of around 200 μΩ-cm. As expected, given the similar XRD results, the resistivity values are very close for 40%, 50% and 60% oxygen and at about 150 μΩ-cm. As reported elsewhere, the resistivity decreased as percent oxygen increased.

Film adhesion results are shown in Table 2. The adhesion of RuO_2 to SU8 was comparable to that of SU8 to silicon, both of which being above 1000 psi. The film deposited with 60% oxygen had the lowest film adhesion, around 700 psi, most likely due to an increase in stress in the film. Overall, the films made with between 30 and 50 percent oxygen gave the best results, with low resistance and high adhesion. Additional effort to measure the electrochemical overpotential for RuO_2 films as an electrode material is currently underway.

4. Conclusion

The resistivity and crystallinity of reactively sputter deposited RuO_2 thin films sputtered as a function of oxygen in the sputtering gas was investigated. In addition, the adhesion of RuO_2 thin films to the cured photoresist SU8 was measured. It was found that a change from Ru to RuO_2 films occurs between 20 and 30 percent oxygen in the

plasma and a transition from (110) to (101) orientation in the films occurred between 80% and 90% oxygen. The change from Ru to RuO_2 occurring between 20 and 30% oxygen was further supported by AES results, which indicated a mixture of Ru and RuO_x in the 20% oxygen film. The resistivity of films was a function of oxygen concentration in the sputtering gas. For <10% O_2 the resistivity was consistent with metallic Ru. Above 20% O_2 the RuO_2 resistivity was around 150-200 μΩ-cm. Adhesion of the RuO_2 to SU8 was approximately 1000 psi for O_2 contents of 30-50% but only around 700 psi for films deposited with 60% oxygen. Due to high film stress, films made with over 70% oxygen in the sputtering gas delaminated from the substrate. Collectively, the results indicated that 40-50% oxygen gave best results, with lower resistivity values and high adhesion to SU8.

5. Acknowledgements

This work was supported in part by the National Institute for Health, Grant 1R15EB006611-O1A1

6. References

1. Hong, S.K., J. of App. Phys. 80 (1996) 822.
2. Nougaret, L., et al., Thin Solid Films. 515 (2007) 3971-3977.
3. Belkind, A., et al., Thin Solid Films. 207 (1992) 242-247.
4. Desu, S.B., et al., Thin Solid Films. 350 (1999) 21-29.
5. Kim, H.K., et al., J. of Vac. Sci. & Tech. B. 21 (2003) 949.

6. Kim, H.K., et al., J. of Vac. Sci. & Tech. B. 20 (2002) 1827.

7. Meng, L.J. and M.P. dos Santos, Thin Solid Films. 375 (2000) 29-32.

8. Huang, J.H. and J.S. Chen, Thin Solid Films. 382 (2001) 139-145.

9. Sakiyama, K., et al., J. of Electrochem. Soc. 140 (1993) 834.

10. Lee, W., et al., Electrochem. and Solid-State Letters. 10 (2007) A225.

11. Lee, J., et al., J. of App. Phys. 77 (1995) 5473.

12. Krusin-Elbaum, L., M. Wittmer, and D.S. Yee, App. Phys. Letters. 50 (1987) 1879.

13. Abe, Y., et al., J. of Vac. Sci. & Tech. B. 18 (2000) 1348.

14. Kolawa, E., et al., Thin Sol. Films. 173 (1989) 217-224.

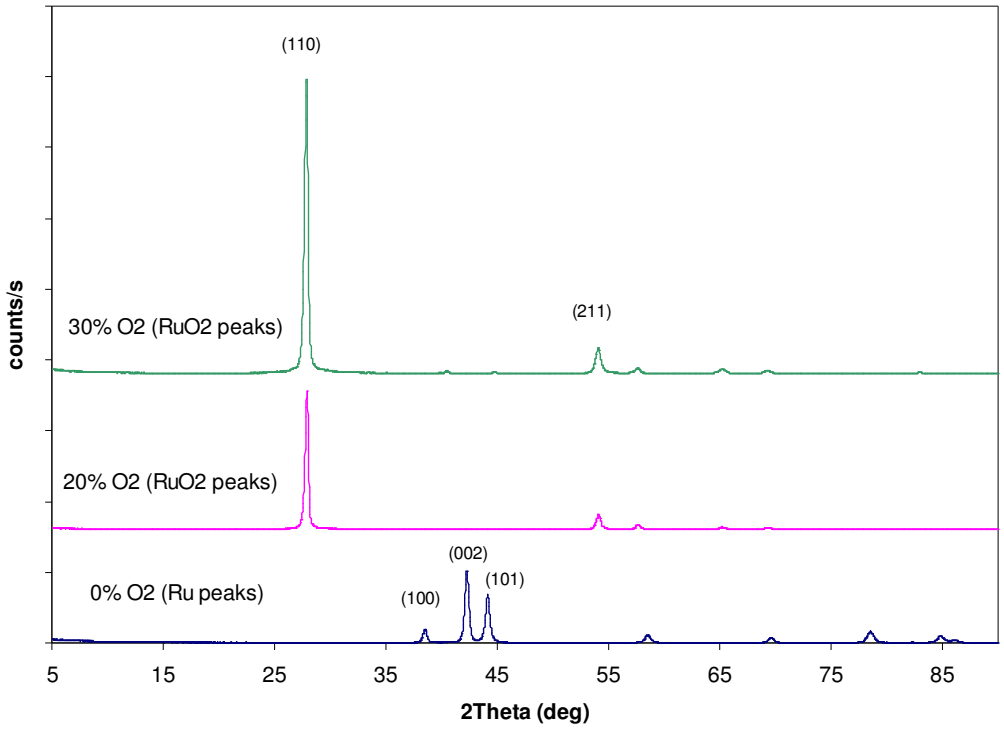

Figure 1. X-ray diffraction spectra of Ru deposited with 0%, 20% and 30% oxygen

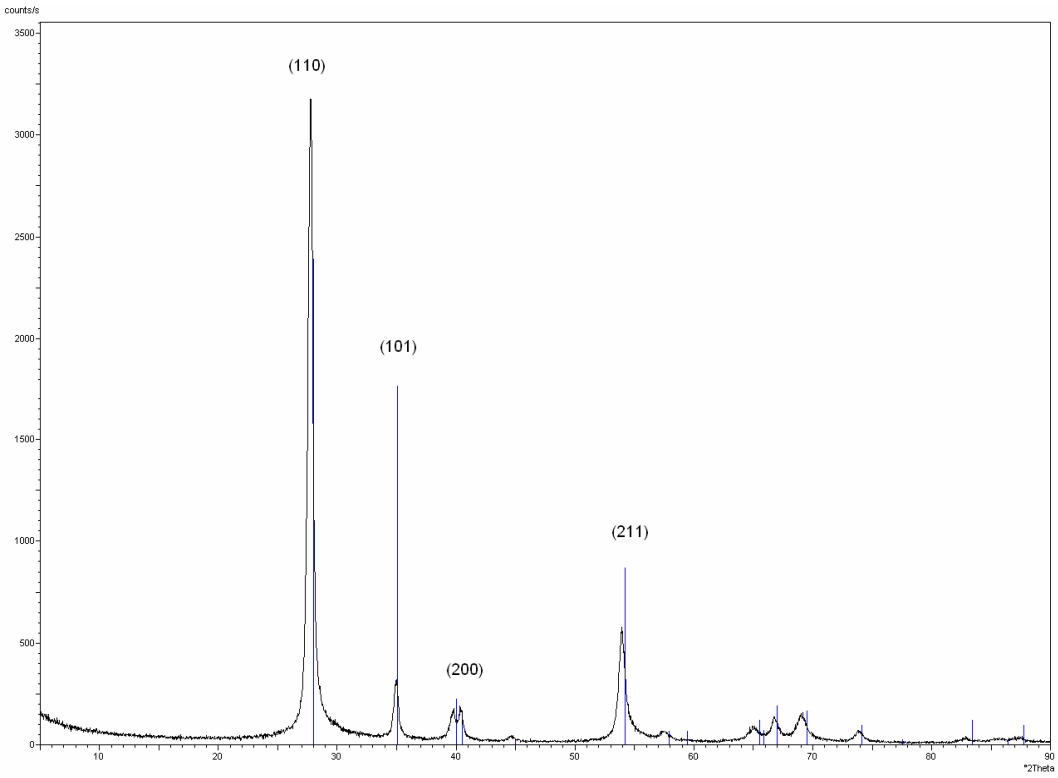

Figure 2. X-ray diffraction spectrum of RuO_2 deposited with 50% oxygen

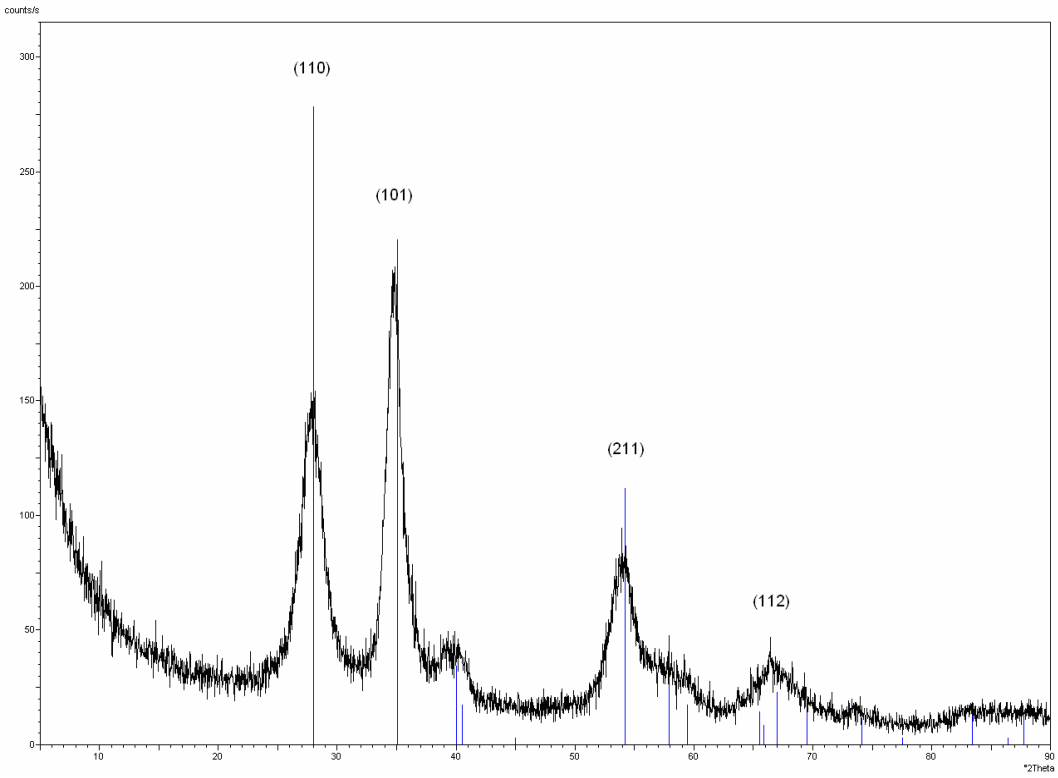

Figure 3. X-ray diffraction spectrum of RuO_2 deposited with 90% oxygen

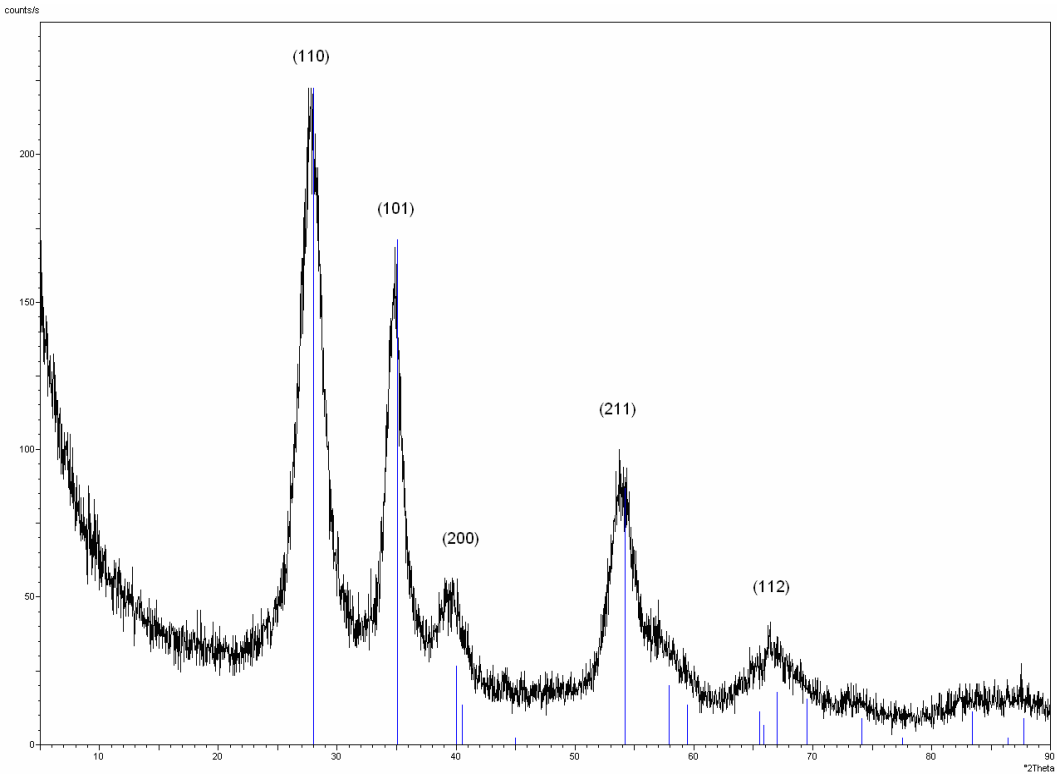

Figure 4. X-ray diffraction spectrum of RuO_2 deposited with 80% oxygen

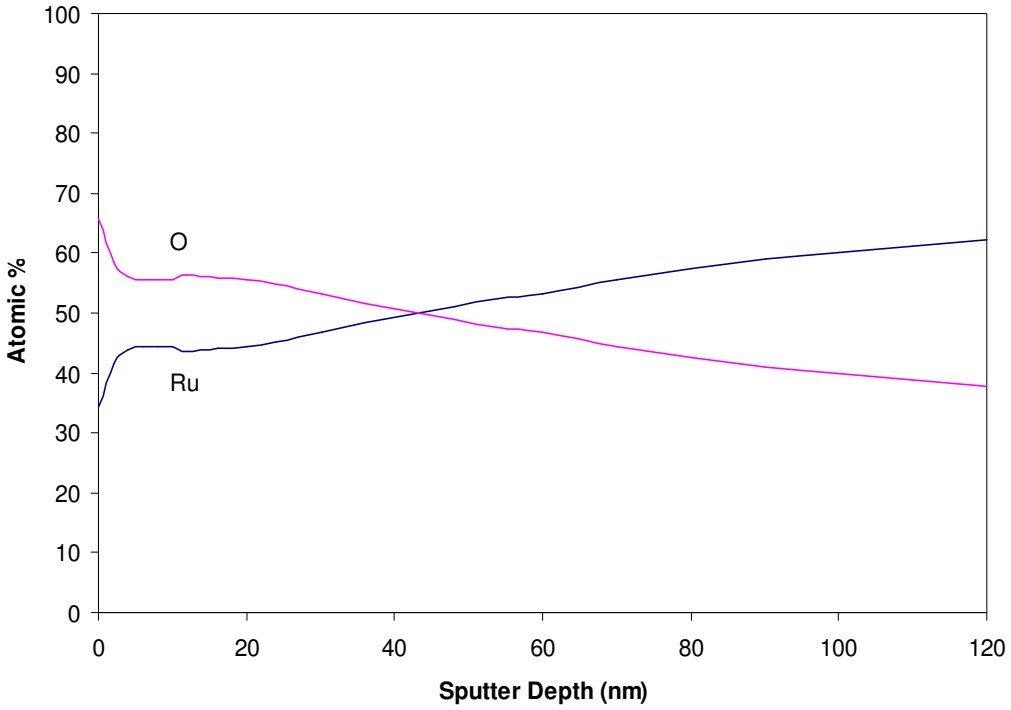

Figure 5. Auger Electron Spectroscopy depth profile of RuO_2 sputtered with 20% oxygen

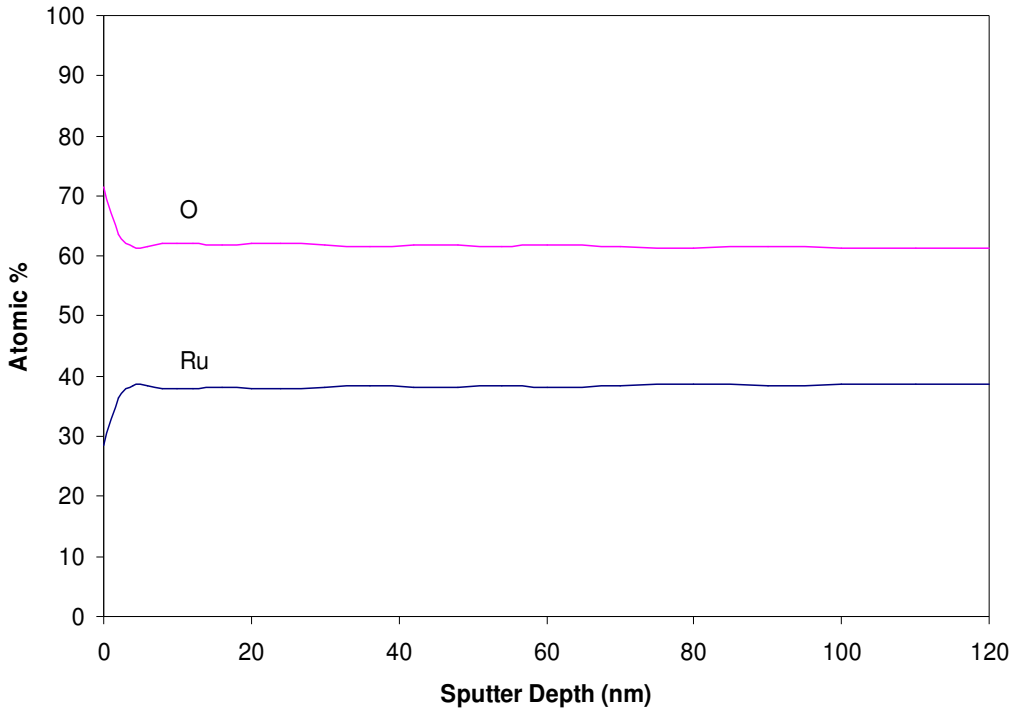

Figure 6. Auger Electron Spectroscopy depth profile of RuO_2 sputtered with 50% oxygen

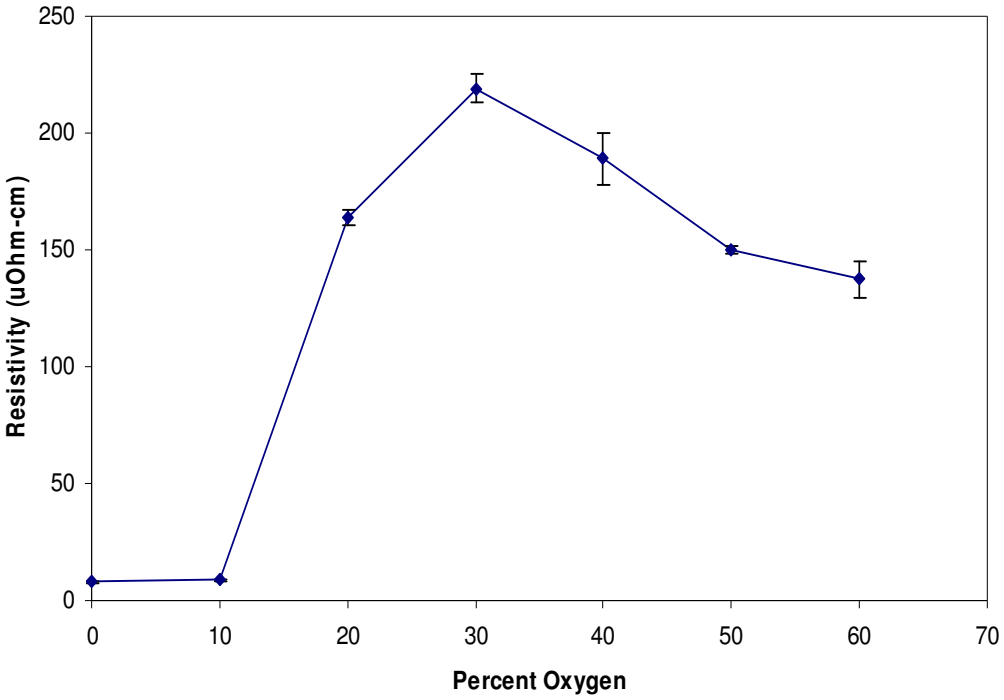

Figure 7. Resistivity for films with various oxygen contents

Table 1. Summary of deposition methods and resistivity of RuO_2 thin films found in the literature

Identifying RuO_2 with	Lowest resistivity ($\mu\Omega$cm)	% O_2	Deposition Parameters	Ref.
XRD, RBS	40	50	500C	[12]
RBS	150	50	200 W, RT	[11]
XRD, RBS	150	50	100W, RT	[14]
XRD	42	20	50W, 500C	[13]
XRD	310	33-65	100W, RT	[8]

Table 2. Film adhesion results

Percent Oxygen	Film Adhesion (psi)
30	1098 ± 145
40	1310 ± 257
50	1371 ± 197
60	730 ± 113

2. CONCLUSIONS

Two materials were investigated for potential use in a self-calibrating biosensor. The first material, SU8, was examined for use in formation of microchannels. Adhesive bonding of partially exposed SU8 to fully exposed SU8 was shown to be an effective method of bonding, with strengths over 1200 psi possible. The data indicate that exposure dose was a more significant parameter than bonding time on the bond strength of SU8 films. Exposure of SU8 to CF_4/O_2 plasmas was also studied. High oxygen plasmas created the most hydrophilic surface when tested with water. The most likely reason high oxygen plasmas make the surface hydrophilic is that the etching would open the epoxy groups, which then can react with O_2 in the environment forming hydrophilic –OH groups on the surface. With less oxygen in the environment, fewer –OH will form, leading to a less hydrophilic surface. The stability of the etched surface was examined through wetting tests over a period of more than one month. For both hydrophobic and hydrophilic samples, the samples with the highest amount of fluorine in the plasma were the most stable over time. Based on the results, microfluidic channels with high bond strengths and hydrophilic surfaces can be realized if the proper processing parameters are selected.

The second material, RuO_2, was investigated as a potential electrode material. It was found that a change from Ru to RuO_2 films occurs between 20 and 30 percent oxygen in the plasma and a transition from (110) to (101) orientation in the films occurred between 80% and 90% oxygen. The change from Ru to RuO_2 occurring between 20 and 30% oxygen was further supported by AES results, which indicated a mixture of Ru and RuO_x in the 20% oxygen film. The resistivity of films was a function

of oxygen concentration in the sputtering gas. For <10% O_2 the resistivity was consistent with metallic Ru. Above 20% O_2 the RuO_2 resistivity was around 150-200 μΩ-cm. Adhesion of the RuO_2 to SU8 was approximately 1000 psi for O_2 contents of 30-50% but only around 700 psi for films deposited with 60% oxygen. Due to high film stress, films made with over 70% oxygen in the sputtering gas delaminated from the substrate. Collectively, the results indicated that 40-50% oxygen gave best results, with lower resistivity values and high adhesion to SU8.

3. FUTURE WORK

There are several experiments that could be done in the future work on this project. The first would be to test the shelf-life of etched SU8 to determine if unused samples maintain there etched chemistry longer than continuously tested ones. The second project would be to fabricate bonded, etched microchannels. A third future project would be to test the overpotential of Ruthenium Oxide.

APPENDIX

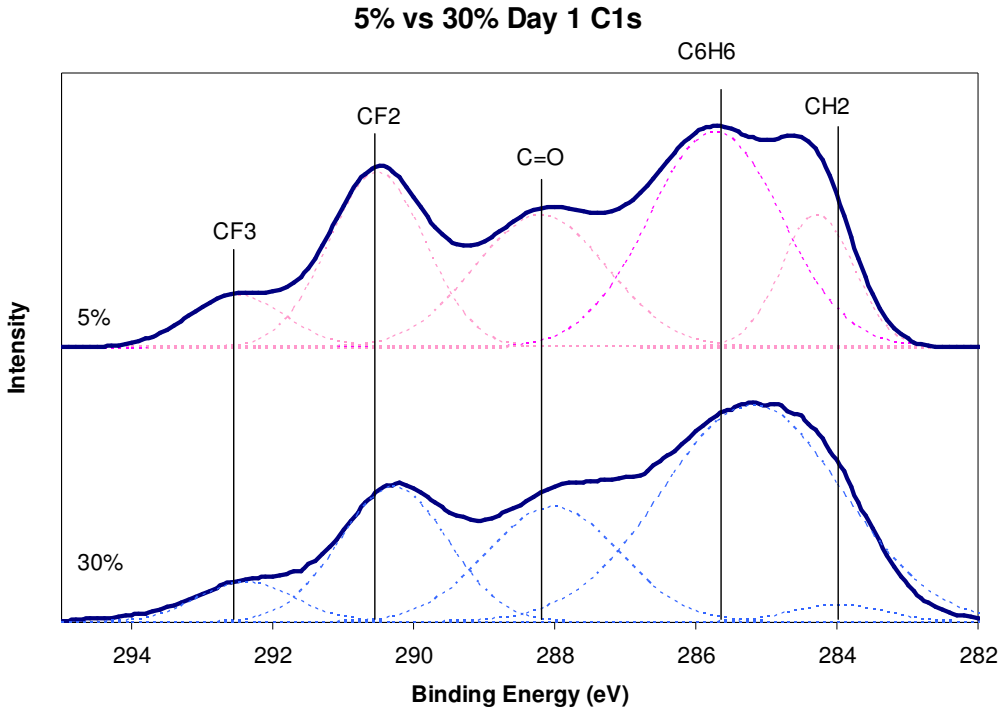
5% vs 30% Day 1 C1s
C6H6
CH2
CF2
C=O
CF3
5%
30%
Intensity
294
292
290
288
286
284
282
Binding Energy (eV)

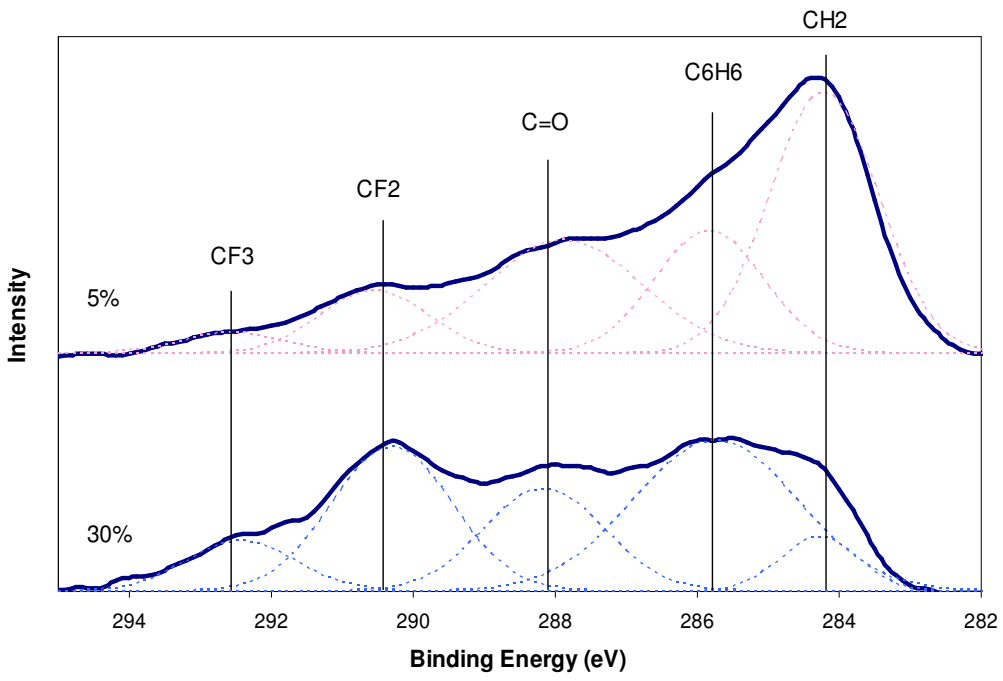
5% vs 30% Day 90 C1s
CH2
C6H6
C=O
CF2
CF3
5%
30%
Intensity
294
292
290
288
286
284
282
Binding Energy (eV)

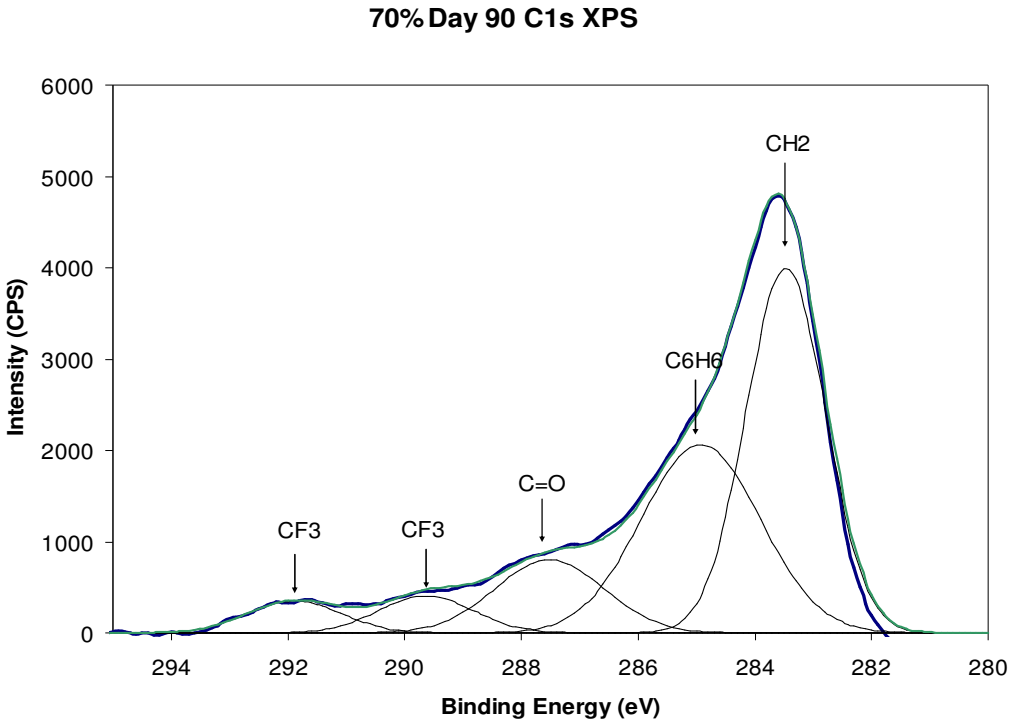
70% Day 90 C1s XPS
Intensity (CPS)
6000
5000
4000
3000
2000
1000
0
294
292
290
288
286
284
282
280
Binding Energy (eV)
CH2
C6H6
C=O
CF3
CF3

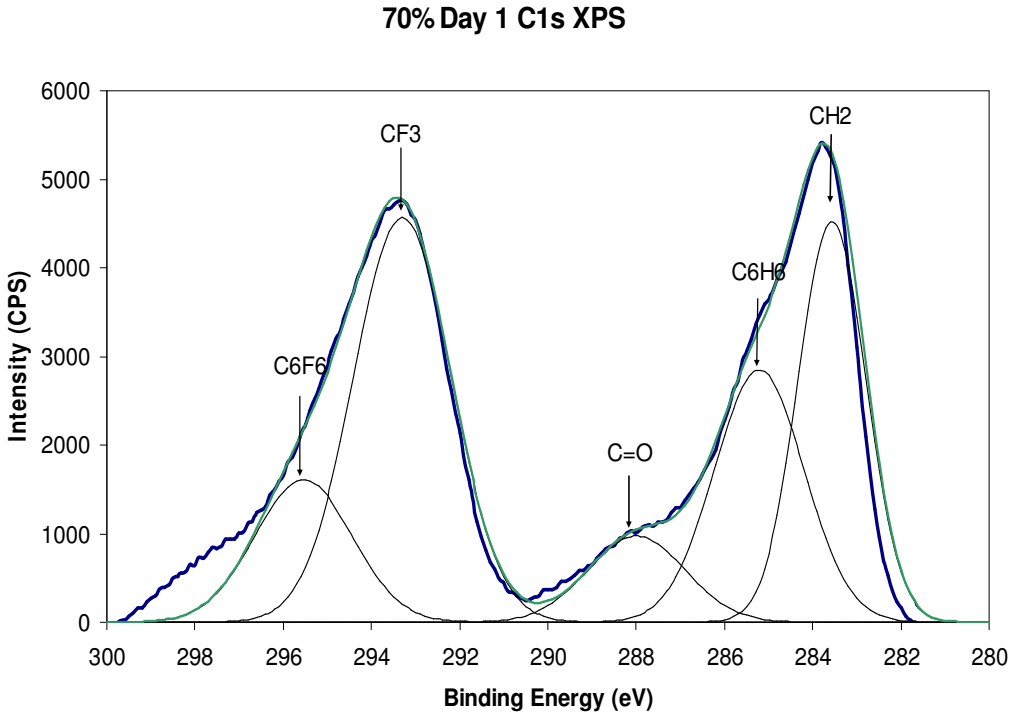
70% Day 1 C1s XPS
Intensity (CPS)
6000
5000
4000
3000
2000
1000
0
300
298
296
294
292
290
288
286
284
282
280
Binding Energy (eV)
CF3
CH2
C6H6
C6F6
C=O

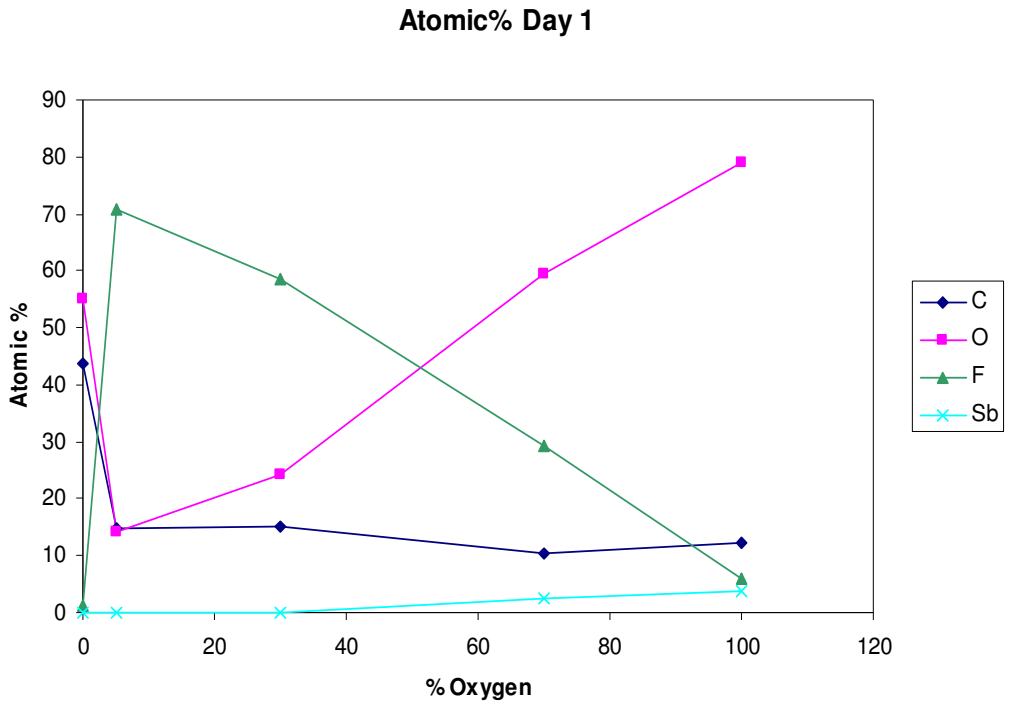
Atomic% Day 1
Atomic %
% Oxygen
C
O
F
Sb
0
10
20
30
40
50
60
70
80
90
0
20
40
60
80
100
120

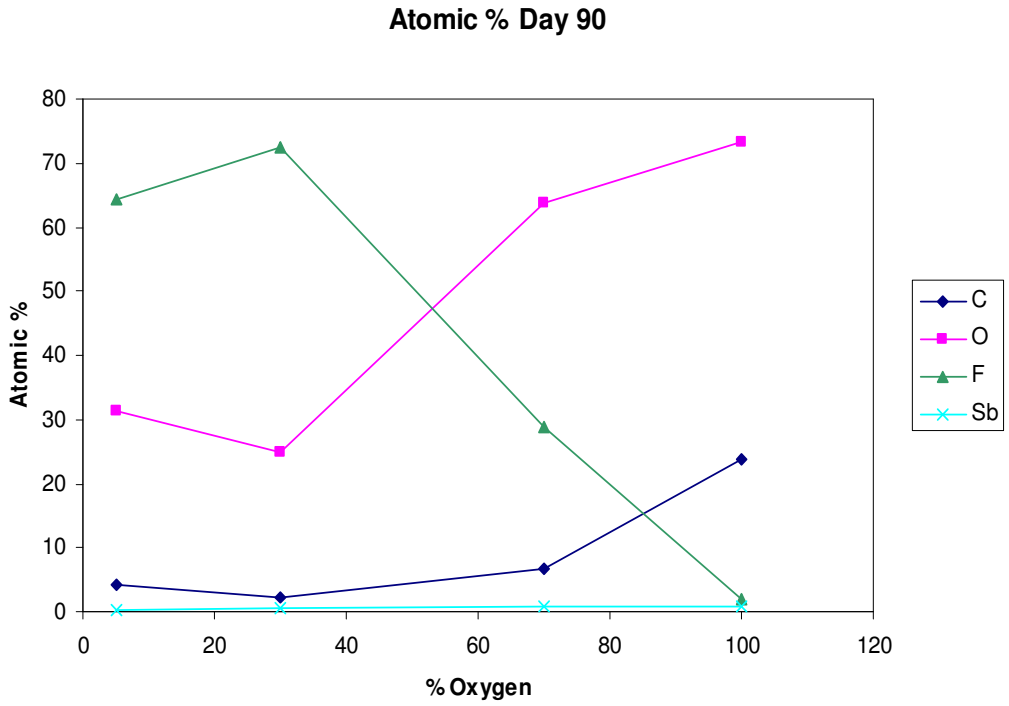
Atomic % Day 90
Atomic %
% Oxygen
C
O
F
Sb
0
10
20
30
40
50
60
70
80
0
20
40
60
80
100
120

VITA

Margaret Theresa Audrain was born in Kansas City, MO on November 16, 1983. She completed high school in Lee's Summit, MO. In the fall of 2002, she began her undergraduate studies at the University of Iowa in Biomedical Engineering. She was a member of the Biomedical Student Society and was an undergraduate research assistant with Dr. Scott Moye-Rowley. Meg graduated in May of 2006.

The following fall, Meg began her graduate studies at the Missouri University of Science and Technology (formerly UMR). She was employed as a graduate research assistant under the direction of Dr. Matt O'Keefe while working on her Master's degree in Materials Science and Engineering.